The 5th Rail Industry Symposium and Exhibition (RISE#5)
Bankkok, 2019-07-11

Development of High corrosion Resistance rail Steel

Prof. Junhua Dong
Institute of Metal Research,
Chinese Academy of Sciences
Shenyang, China

Background

Presently railways rely on a wide variety of steels for its materials requirement. It is since steel meets the requirements of cost, weight, reliability, crashworthiness, maintainability and inspection required by the railways. Large varieties of steels are used by railways for its requirement for

(i) rolling stock (locomotives, coaches, and wagons),

(ii) rail tracks (permanent way),

(iii) electric traction,

(iv) infrastructure.

The quality of steels used are: mild steel, other plain carbon steels, alloy steels, high strength steels, wear resistant steels, corrosion resistant steels, spring steels, electrical steels, and stainless steels etc.

Background

The rail track is known as a stable structure. It ensures the transportation of trains through providing a dependable surface for their wheels.

Rail track can be divided into main four components namely

(i) rails,

(ii) sleepers,

(iii) fish plates,

(iv) rail fasteners.

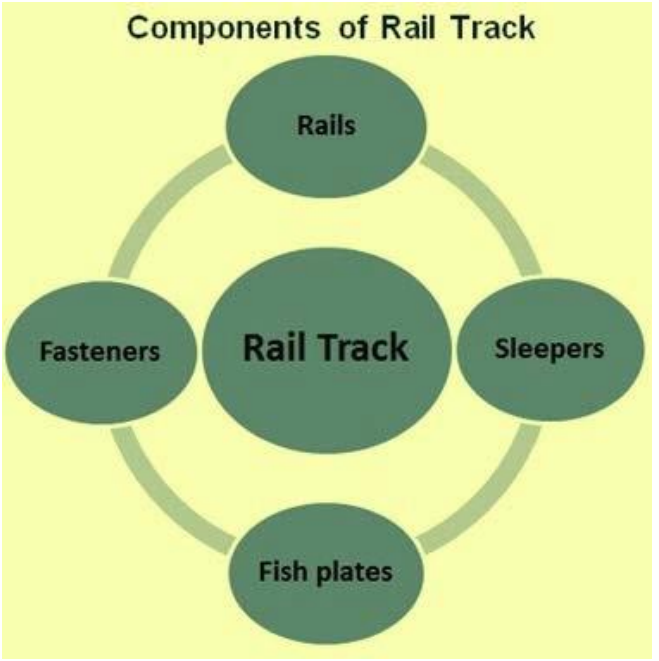

Background

Rail is the most expensive material in the track. Rail is the steel section that has been rolled into an inverted T shape.

Rails are made of high carbon steel to be able to withstand stresses:

(C: 0.6 ~ 0.8, Mn: 0.8 ~ 1.3, Si: 0.1 ~ 0.5 , S < 0.03, P < 0.03, Al< 0.015).

Some grades of steel contain chromium (Cr: 0.8 ~ 1.2).

Rails are also produced from special steels containing :

niobium (Nb- 0.04 % max.) or vanadium (V-0.2 % max.).

Recently rails made from corrosion resistant steels have also been developed.

The corrosion types in a rail section include:

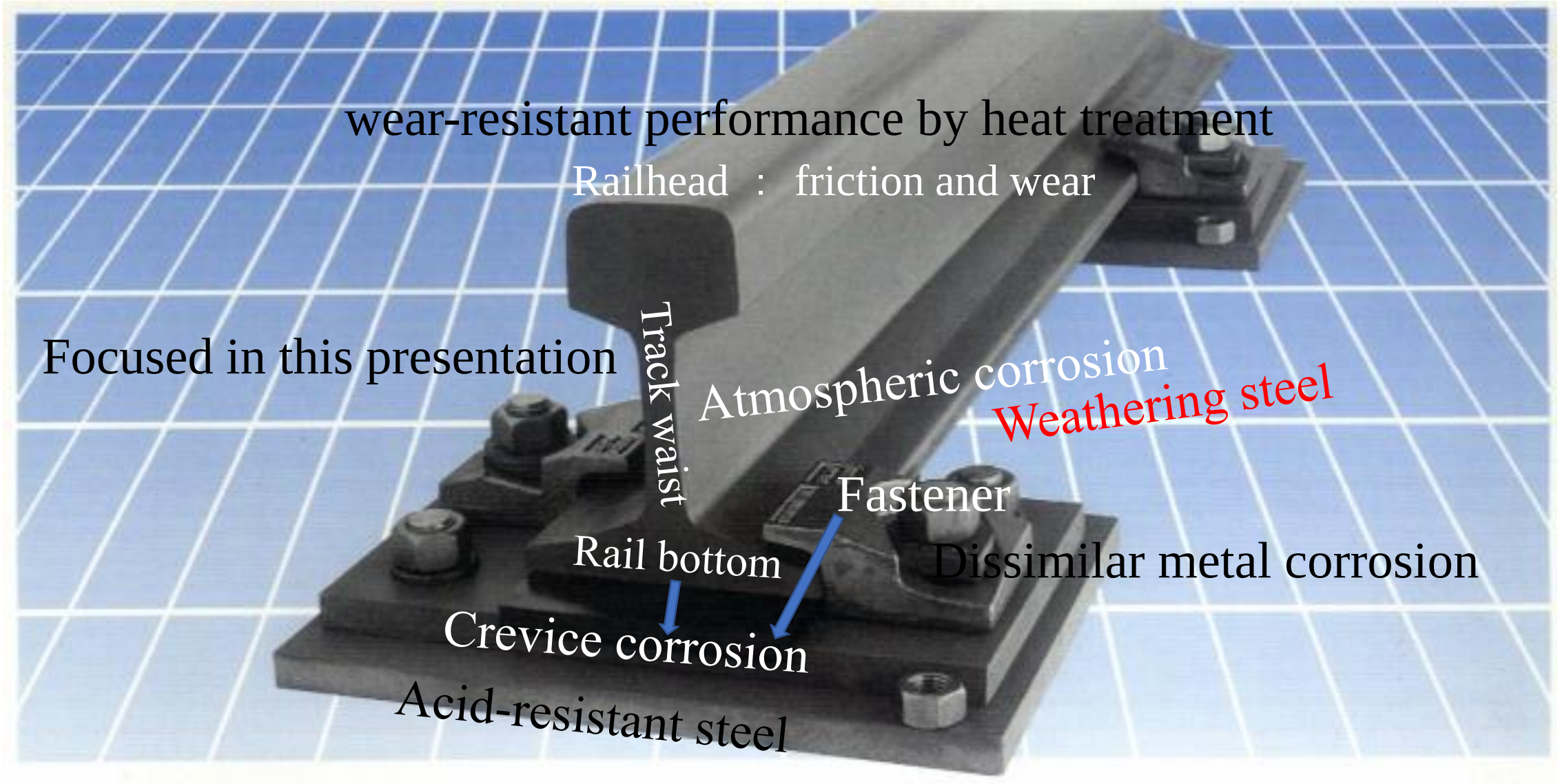

Alloy development of corrosion-resistant rail steel

R. Balasubramaniam[1,†], B. Panda[1], G. Dwivedi[1], A. P. Moon[1,*], S. Mahapatra[1], A. K. Manuwal[2], A. Bhattacharyya[3], K. Srikanth[3] and R. K. Rathi[4]

[1]Department of Materials Science and Engineering, Indian Institute of Technology, Kanpur 208 016, India
[2]Research Designs and Standards Organization, Indian Railways, Manaknagar, Lucknow 226 011, India
[3]Research and Development Centre for Iron and Steel, Steel Authority of India, Doranda, Ranchi 834 002, India
[4]Steel Melting Shop and Research Control Laboratory, Bhilai Steel Plant, Bhilai 490 001, India

Table 1. Chemical composition of C–Mn, Cu–Mo and the four new rail steels

Sample	C	Mn	Cu	Mo	Cr	Ni	Si	S	P
C–Mn	0.71	1.04	–	–	–	–	0.21	0.013	0.022
Cu–Mo	0.69	1.16	0.24	0.18	–	–	0.19	0.022	0.024
Cu–Si	0.60	1.20	0.35	–	–	–	0.66	0.024	0.027
Cu–Ni	0.63	1.02	0.41	–	–	0.20	0.31	0.020	0.028
Cr–Cu–Ni	0.71	1.15	0.40	–	0.59	0.20	0.35	0.026	0.027
Cr–Cu–Ni–Si	0.70	1.09	0.39	–	0.53	0.20	0.56	0.023	0.027

Figure 1. Arrangement for conducting crevice corrosion test according to ASTM G-78: *a*, Unassembled components and *b*, Assembled condition.

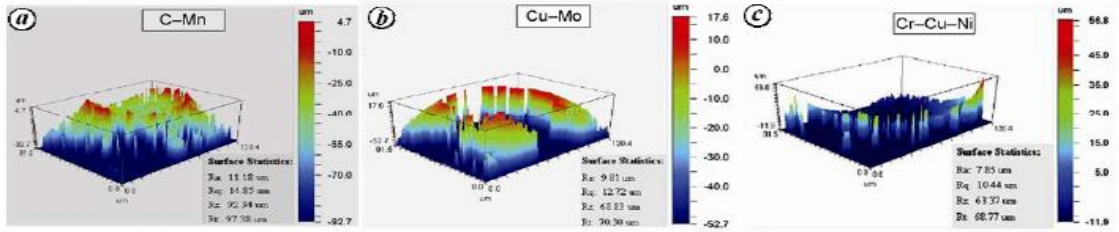

Figure 2. Typical results from profilometer analysis at the starting portion of the crevice (location 1). *a*, C–Mn steel sample; *b*, Cu–Mo and *c*, Cr–Cu–Ni rail steel sample on immersion in 3.5% NaCl + 3.5% $FeCl_3$ solution after 30 days.

Table 2. Average surface roughness (μm) at three locations on the crevice created in rail steels after immersion in 3.5% NaCl + 3.5% $FeCl_3$ solution after 30 days of immersion

	Location		
Metal	3	2	1
C–Mn	3.87	3.43	12.41
Cu–Mo	2.61	2.73	9.70
Cr–Cu–Ni	2.09	2.47	7.85

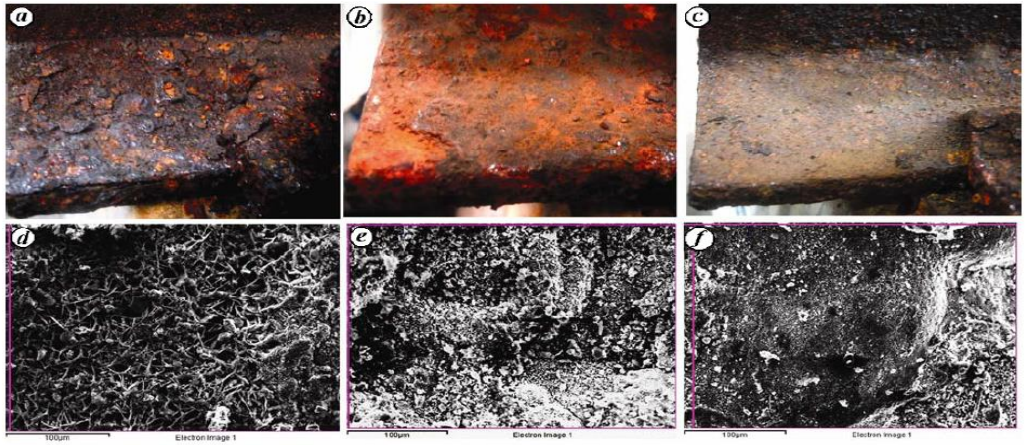

Figure 3. Macro images of foot portion of rail steel: *a*, C–Mn; *b*, Cu–Mo and *c*, Cr–Cu–Ni and corresponding microscopic features (observed by SEM) of outer rust on the rail steels. *d–f*, After six months of salt fog exposure showing the lower rusting and compact rust formation in the case of Cr–Cu–Ni rail steel.

Atmospheric corrosion evolution of Low Alloy Steel (LAS)

Initial stage:
The adsorption and absorption of water

Middle stage:
The deposition of gaseous phase, The chemical changes in the liquid phase, and the dissolution of steel.

Final stage:
The aggregation, growth, and thickening of the corrosion product.

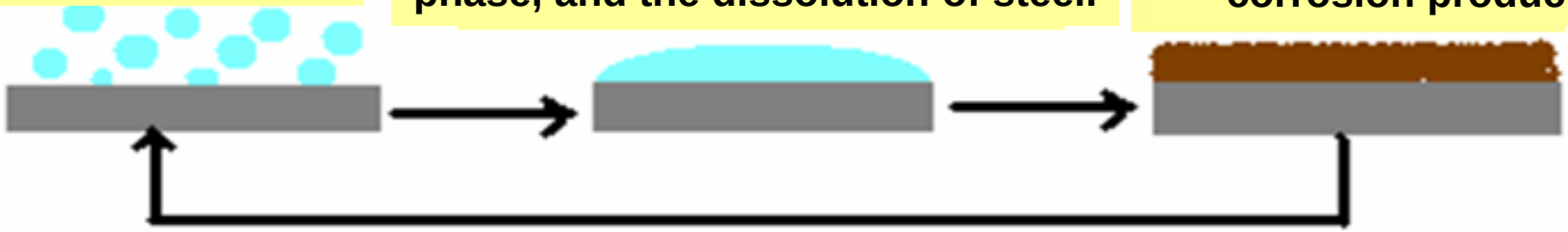

* *C. Leygraf, T. E. Graedel, Atmospheric Corrosion*

the initial stage and the middle stage experienced very short time, even within 1 wet/dry cycle. **The final stage** occupied most of the service time.

Atmospheric corrosion evolution of Low Alloy Steel (LAS)

Anode of corrosion

$$Fe_{(M)} = Fe^{2+}_{(sol)} + 2e_{(M)}$$

Hydrolysis and the subsequent oxidation

Cathode of corrosion

Initial and middle stages

$$O_{2(g)} + 2H_2O + 4e_{(M)} = 4OH^-_{(sol)}$$

The final stage

$$8FeOOH + Fe^{2+} + 2e = 3Fe_3O_4 + 4H_2O$$

- Atmospheric corrosion evolution of LAS is correlated with the rust compositions of α-FeOOH, β -FeOOH, γ -FeOOH, and Fe_3O_4.
- Alloy elements and the environmental type make significant impact on the rust composition.

Atmospheric corrosion evolution of Low Alloy Steel (LAS)

1. Industrial (SO_2): α- or γ- FeOOH
2. Coastal (Cl^-): β -FeOOH
3. Industrial – coastal (SO_2+ Cl^-) correlate with each content

1. Weathering steel: Cu, P, Cr, Ni, Mo, Si, …

Cu: Fe_3O_4; Ni: Fe_3O_4,α- FeOOH;

Cr: α- FeOOH; Mn-Cu: Fe_3O_4, γ -FeOOH

Misawa, T., Asami, K., Hashimoto, K., and Shimodaira, S., Corr. Sci., vol. 14, pp. 131-149, 1974.

Kamimura, T., Hara, S., Miyuki, H., Yamashita, M., and Uchida, H., Corr. Sci., vol. 48, pp. 2799-2812, 2006.

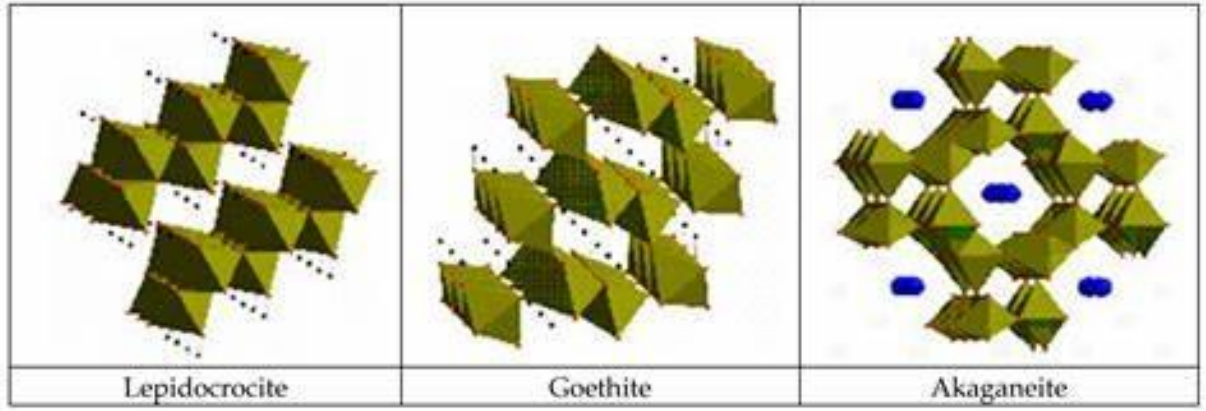

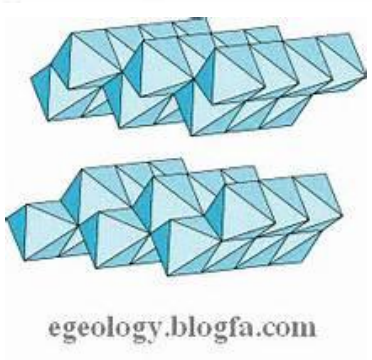

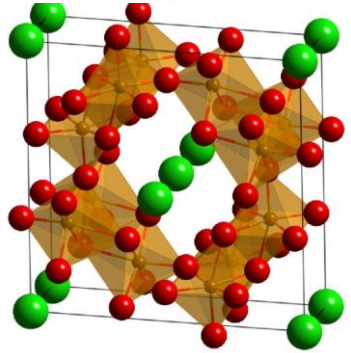

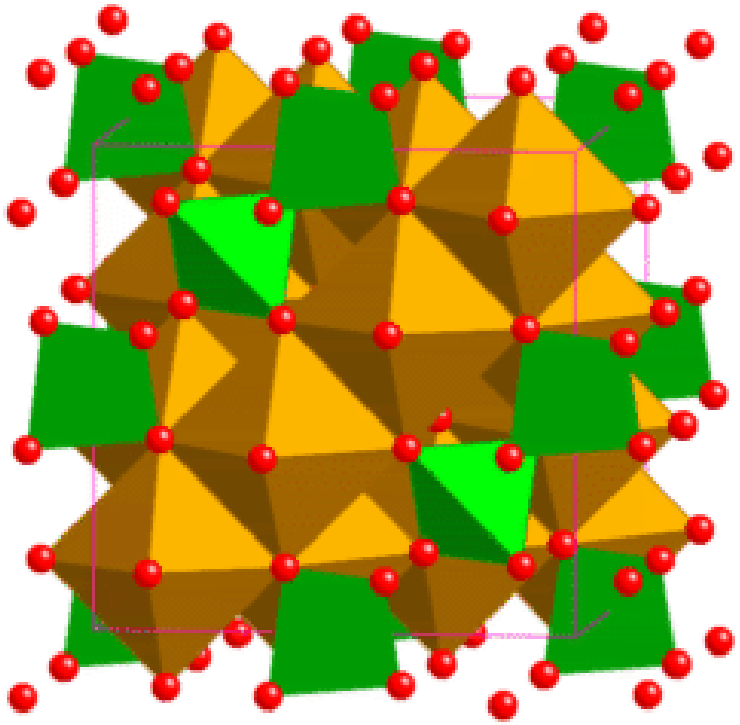

The difference of reduction ability for α-FeOOH, γ -FeOOH and β -FeOOH

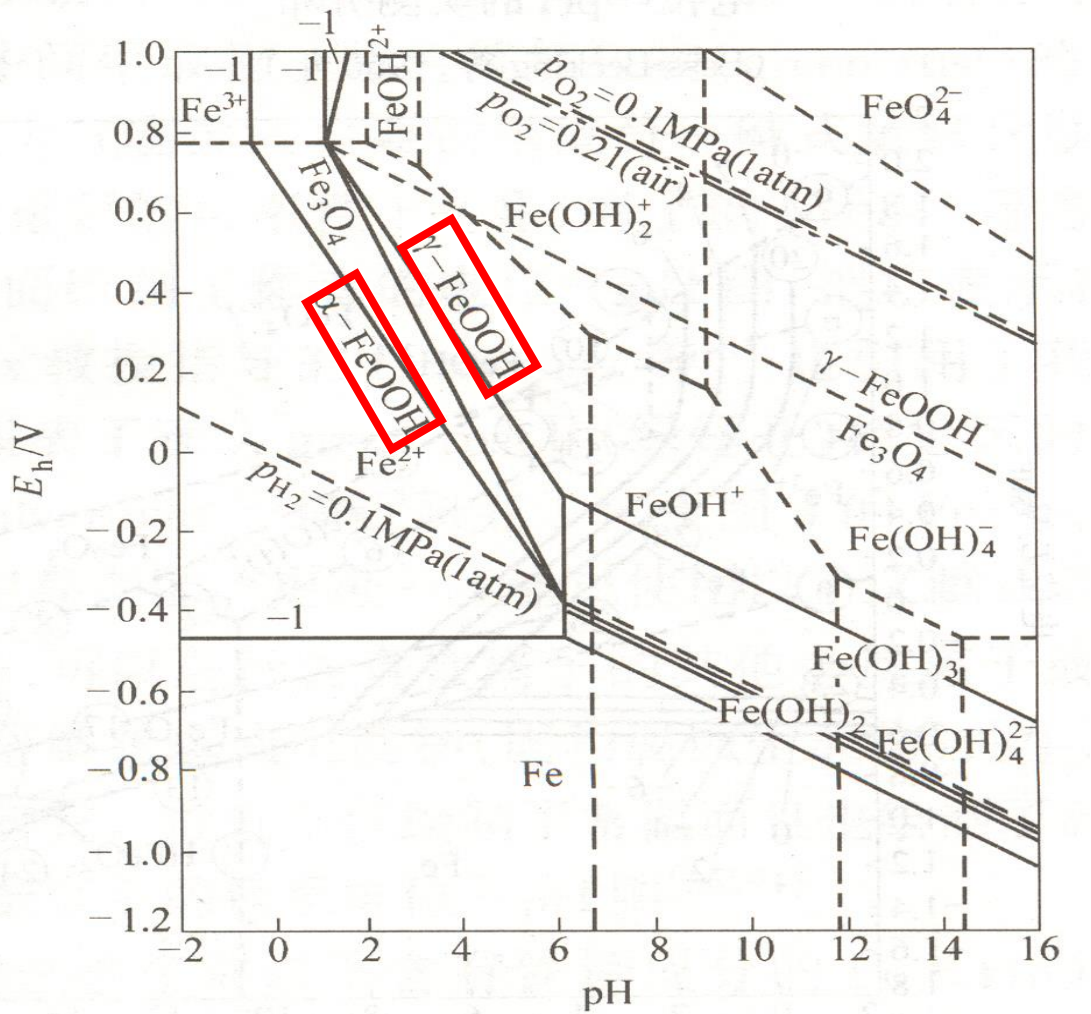

- The stability of the ferric hydroxides : α-FeOOH, γ -FeOOH, β -FeOOH
- the corrosion decelerating compositions: α-FeOOH and Fe_3O_4
- the corrosion accelerating compositions: γ -FeOOH and β -FeOOH
- Protective Ability Index (PAI) α/γ* = α-FeOOH/(β-FeOOH+γ-FeOOH+Spinel)

M. Pourbaix, Atlas of Electrochemical Equilibria in Aqueous Solutions, NACE-Cebelcor(1974)

Yamashita, M., Miyuki, H., Matsuda, T., Nagano, H., and Misawa, T., Corr. Sci., vol. 36, pp. 283-299, 1994.

W. Ke, J.H. Dong, Acta Metal. Sin. 46 (2010) 1365-1378.

L. Hao, S.X. Zhang, J.H. Dong, W. Ke, Corros. Sci. 58 (2012) 175-180.

Outdoor atmospheric corrosion exposure test and its indoor simulated corrosion acceleration test

循环温度：30° C

相对湿度：60%

循环周期：12hrs

模拟介质：

0.3% NaCl；海岸大气

0.052% $NaHSO_3$（pH4）；

工业酸雨大气

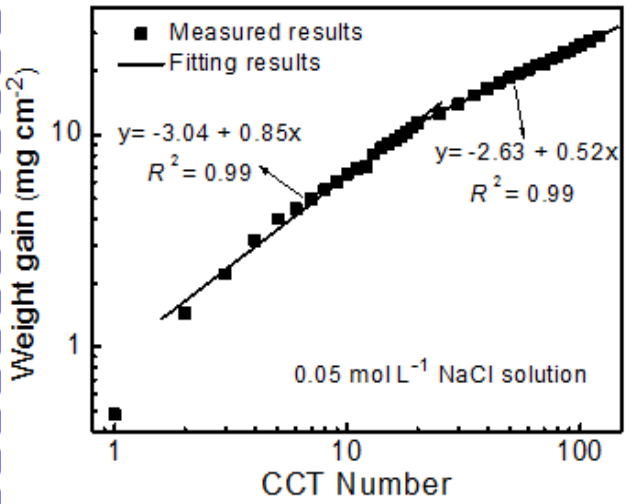

年平均温度 ℃	24.8
年平均相对湿度%	87
年日照时数 h	2154.4
总辐射量MJ/m²	4825.5
年降雨量 mm	1941.5
降水 pH值	5.4
SO₂mg/100cm².d	0.0425
气候特征	高温高湿海洋气候

万宁站

Relevant

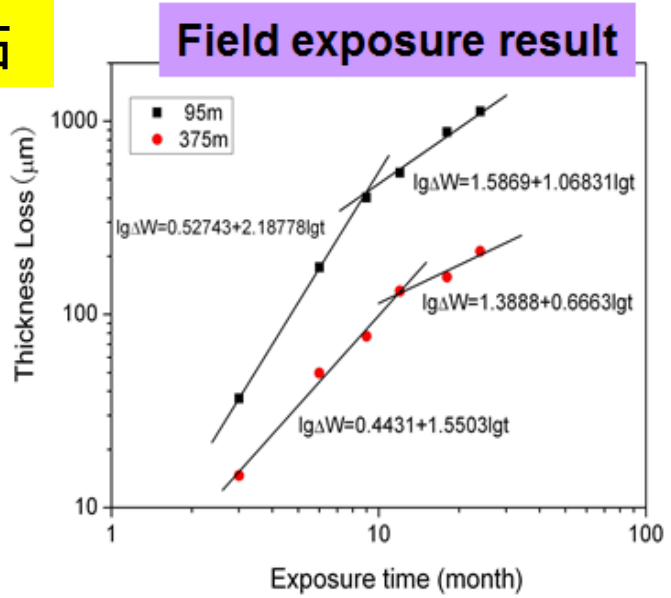

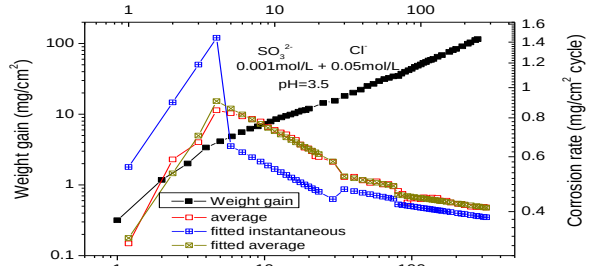

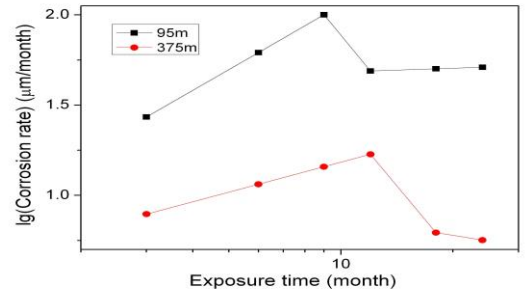

$$\Delta W = At^n$$

$$\Delta W / t = At^{n-1}$$

$$dW / dt = Ant^{n-1}$$

Fitting of atmospheric corrosion evolution

$$\Delta W = At^n$$

$$\Delta W/t = At^{n-1}$$

$$dW/dt = Ant^{n-1}$$

- *power model* (linear bilogarithmic law):

1. *Weight loss:*

   $lg(\Delta W) = A + n lg(t)$

2. *Mean corrosion rate:*

   $lg(\Delta W/t) = A + (n-1) lg(t)$ can be fitted by data

3. Instantaneous corrosion rate

   $lg(d\Delta W/dt) = A + lg(n) + (n-1) lg(t)$ can notm just calculate

A: the initial mean corrosion rate;

A + 1g(n): the initial Instantaneous corrosion rate;

n or *(n-1):* a measure of the long-term change in corrosion rate.

n>1: corrosion accelerated; n<1: corrosion decelerated

- *the sign of (n-1) is correlated with the type of ferric hydroxides*

In case of oxygen diffusion

In the case of the atmospheric corrosion starts on a steel substrate, the cathodic current density of oxygen reduction reaction (equation 4) equals to the diffusion limited current density (I_L) of oxygen.

$$O_2 + 2H_2O + 4e = 4OH^-$$

$$d\Delta W/dt = z_i F I_c \qquad I_c = I_L$$

If the corrosion is always controlled by the limited diffusion of oxygen, the corrosion rate will keep as a constant (I_L)

$$n - 1 = 0$$

In case of goethite reduction

$$8\alpha\text{-FeOOH} + Fe^{2+} + 2e = 3Fe_3O_4 + 4H_2O$$

$$d\Delta W/dt = zFI_c = z_iF(1-\theta_{\alpha\text{-FeOOH}}-\theta_{Fe3O4})I_L + z_jF\theta_{\alpha\text{-FeOOH}}I_{c\text{-}\alpha}$$

$$z_j\theta_{\alpha\text{-FeOOH}}I_{c\text{-}\alpha\text{-FeOOH}} - z_i(\theta_{\alpha\text{-FeOOH}}+\theta_{Fe3O4})I_L < 0$$

then $I_c < I_L$, and I_c reduces with the increase of $\theta_{\alpha\text{-FeOOH}} + \theta_{Fe3O4}$, *in other words,* I_c *decreases with the extension of time.*

$$n-1<0$$

www.imr.cas.cn

Evolution of mass loss and rust composition

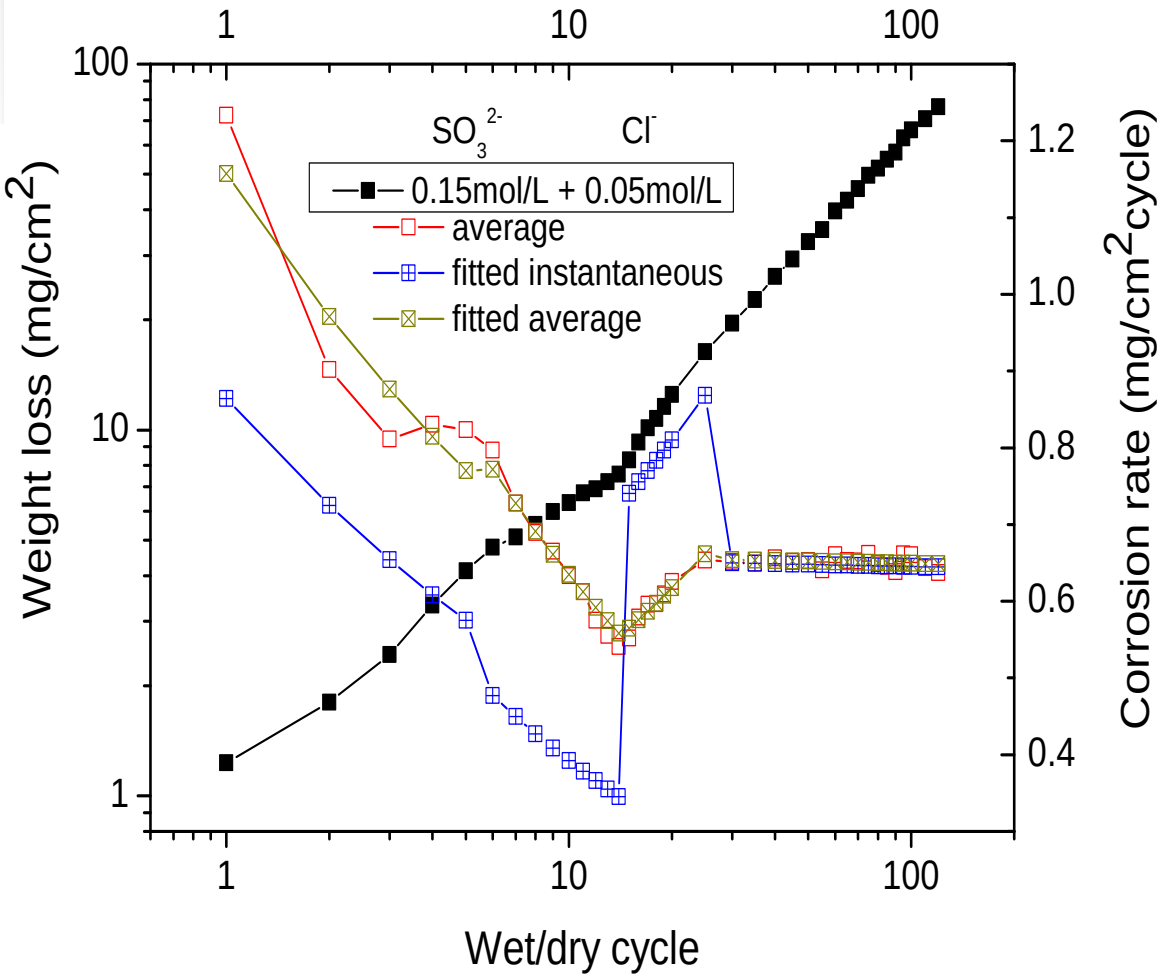

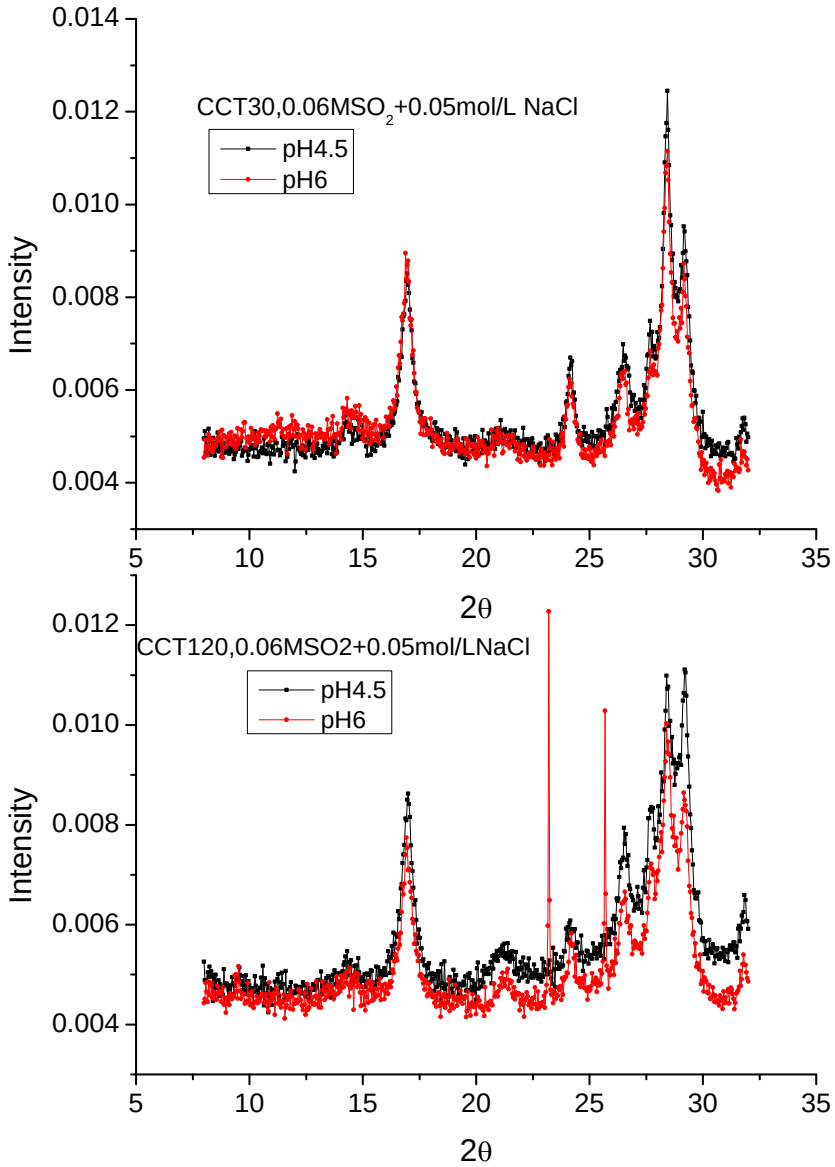

In case of γ-FeOOH reduction

$$8\ \gamma\text{- FeOOH} + Fe^{2+} + 2e = 3Fe_3O_4 + 4H_2O$$

$$d\Delta W/dt = zFI_c = z_iF(1-\theta_{\gamma\text{-}FeOOH}-\theta_{Fe3O4})I_L + z_jF\theta_{\gamma\text{-}FeOOH}I_{c\text{-}\gamma\text{- FeOOH}}$$

$$z_j\theta_{\gamma\text{-}FeOOH}I_{c\text{-}\gamma\text{-}FeOOH} - z_i(\theta_{\gamma\text{-}FeOOH}+\theta_{Fe3O4})I_L > 0 \qquad I_c > I_L$$

I_c increases with the increase of $\theta_{\gamma\text{-}FeOOH}$, *that means* I_c *increases with time extension in the initial stage.*

$$n-1>0.$$

while θ_{Fe3O4} *increases with the reduction of* γ- FeOOH, which again reduces I_c with the *extension of time.*

$$when\ I_c < I_L,\ n-1<0$$

In case of existing both α- FeOOH and γ- FeOOH

$$d\Delta W/dt = zFI_c$$

$$= z_iF(1-\theta_{\alpha\text{-}FeOOH}-\theta_{\gamma\text{-}FeOOH}-\theta_{Fe3O4})I_L +$$

$$z_jF(\theta_{\gamma\text{-}FeOOH}I_{c\text{-}\gamma\text{-}FeOOH} + \theta_{\alpha\text{-}FeOOH}I_{c\text{-}\alpha\text{-}FeOOH})$$

$$z_j(\theta_{\gamma\text{-}FeOOH}I_{c\text{-}\gamma\text{-}FeOOH} + \theta_{\alpha\text{-}FeOOH}I_{c\text{-}\alpha\text{-}FeOOH})-$$

$$z_i(1-\theta_{\alpha\text{-}FeOOH}-\theta_{\gamma\text{-}FeOOH}-\theta_{Fe3O4})I_L>0$$

$$n-1>0$$

$$z_j(\theta_{\gamma\text{-}FeOOH}I_{c\text{-}\gamma\text{-}FeOOH} + \theta_{\alpha\text{-}FeOOH}I_{c\text{-}\alpha\text{-}FeOOH})-$$

$$z_i(1-\theta_{\alpha\text{-}FeOOH}-\theta_{\gamma\text{-}FeOOH}-\theta_{Fe3O4})I_L<0, .$$

$$n-1<0$$

www.imr.cas.cn

Evolution of mass loss and rust composition

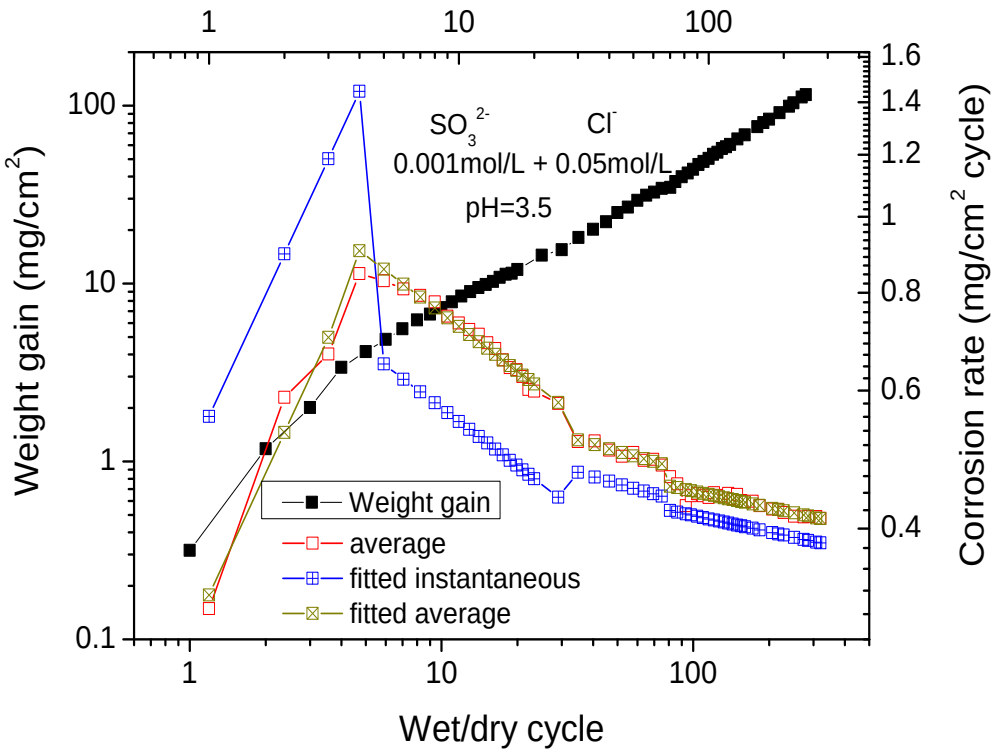

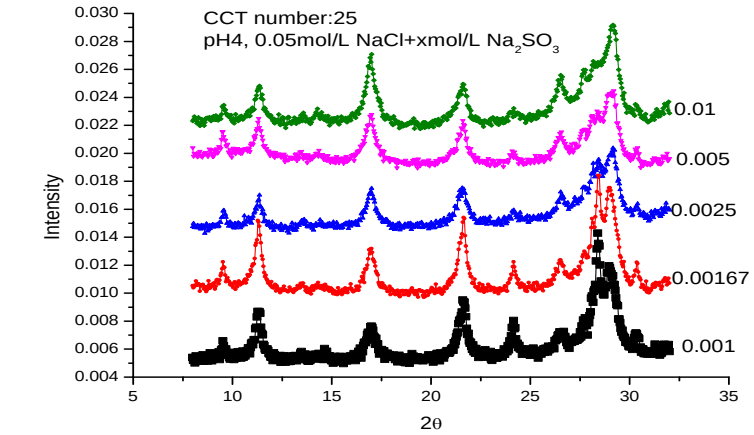

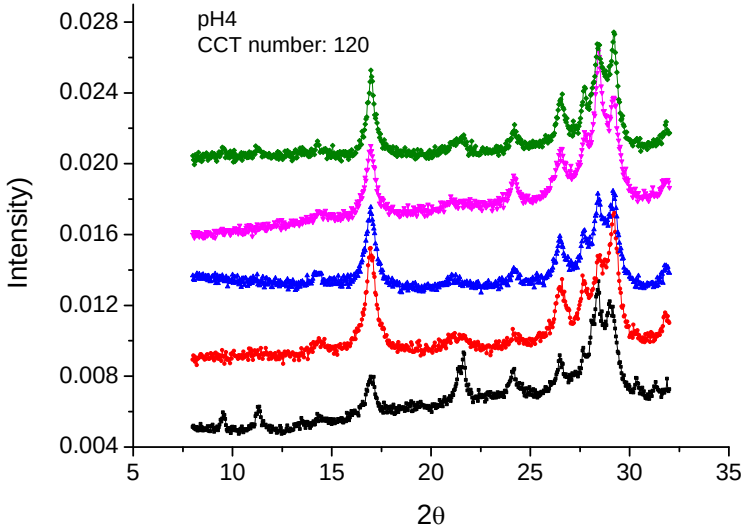

www.imr.cas.cn

Corrosion Evolution of Q235 Steel under the Simulated Wet/Dry Cyclic Corrosion Test

（0.3%NaCl）

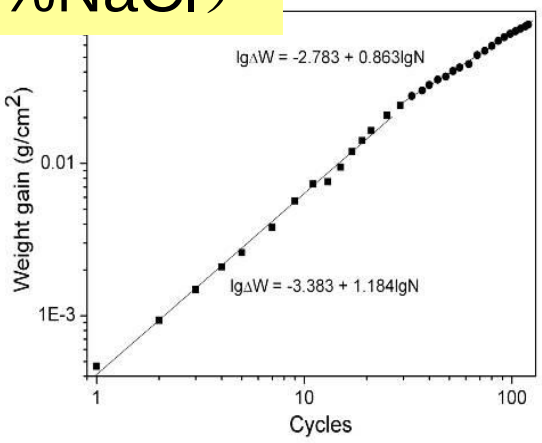

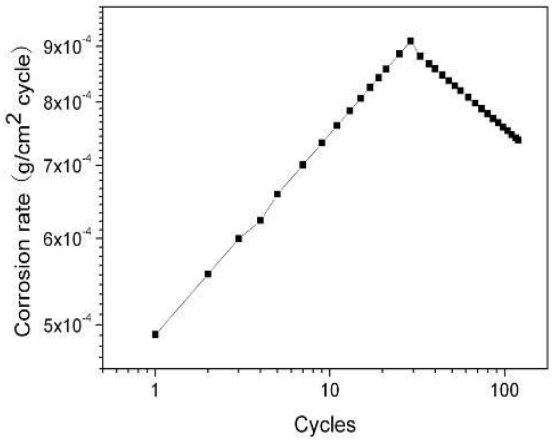

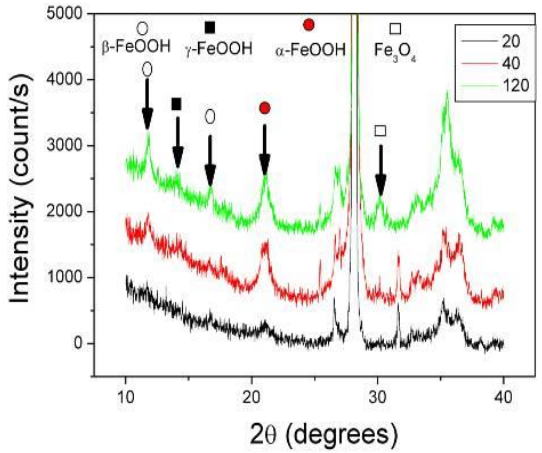

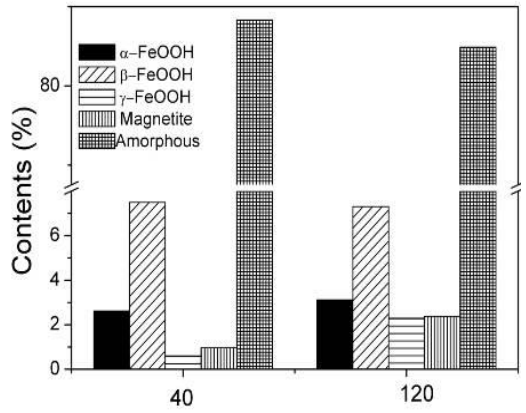

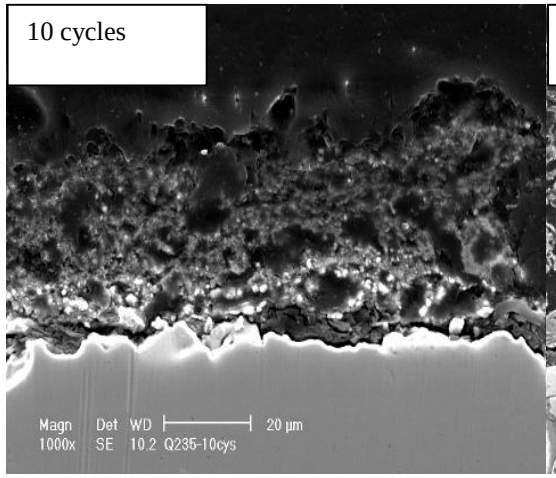

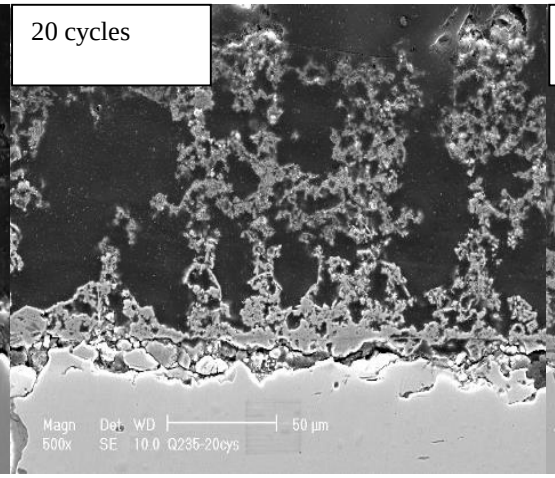

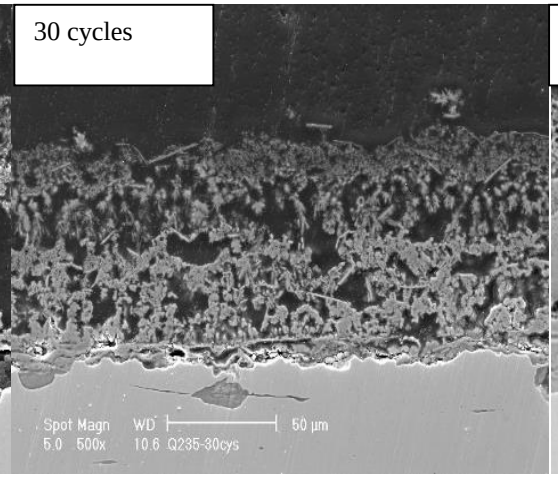

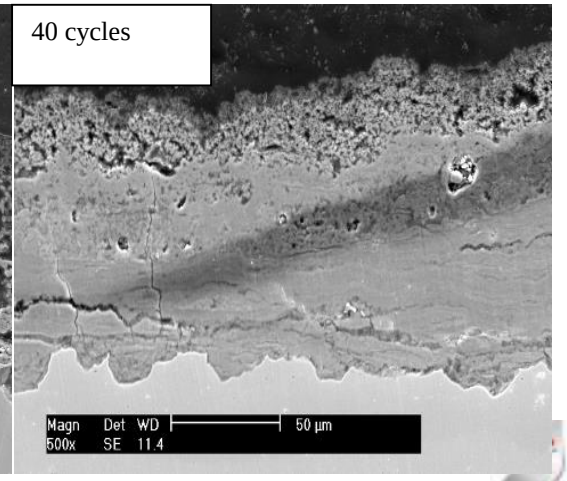

$$\log\Delta W = \log(A) + (n)\log t; \quad \frac{d\Delta W}{dt} = Ant^{n-1}; \quad \log\frac{d\Delta W}{dt} = \log(An) + (n-1)\log t$$

www.imr.cas.cn

Mn-Cu weathering steel: evaluation in simulated coastal environment

（0.3%NaCl）

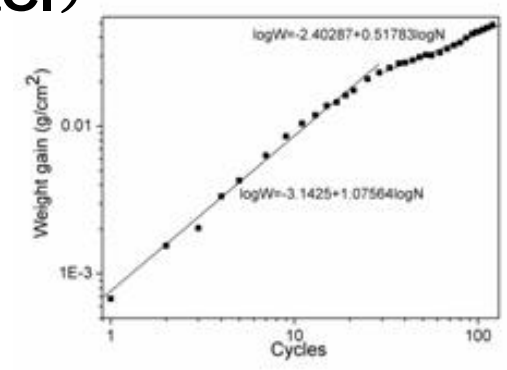

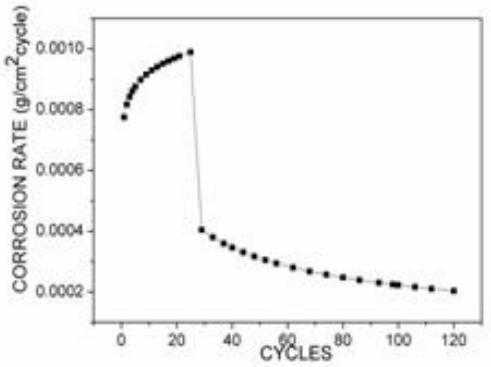

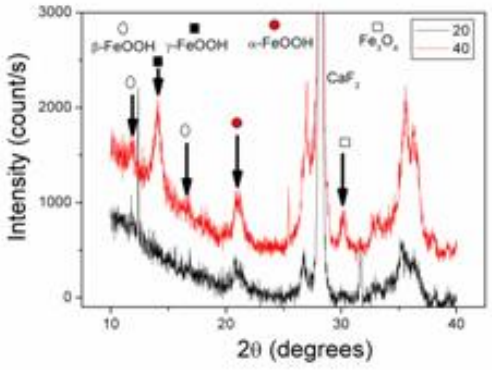

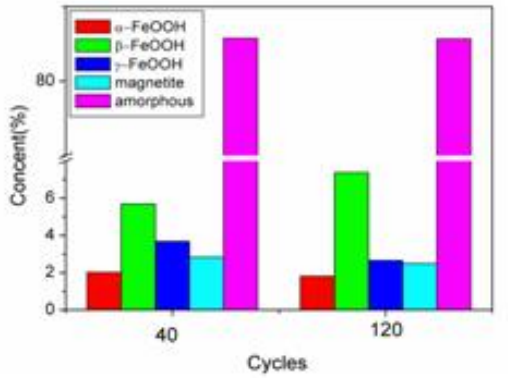

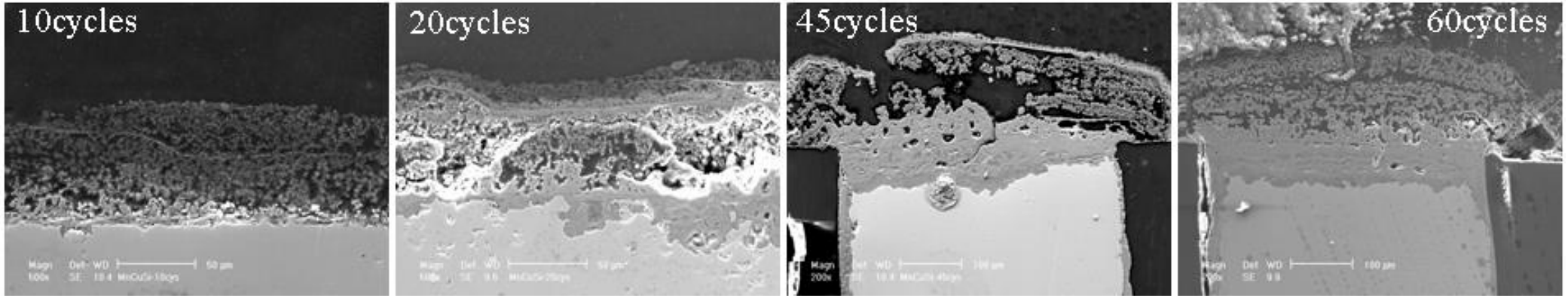

$lg\Delta W = lgA + nlgt$

$$\frac{dW}{dt} = Ant^{n-1}$$

Turning point moved up! moves up to form!

γ-FeOOH and Fe_3O_4 moved up to occur! Compact rust

Relationships of rust composition/structure and its properties of weathering

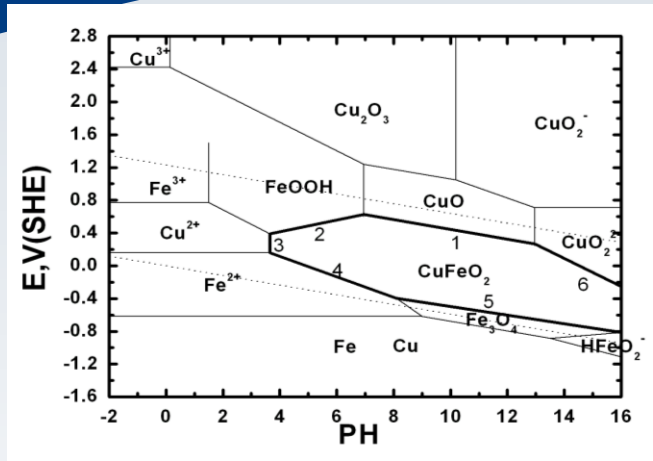

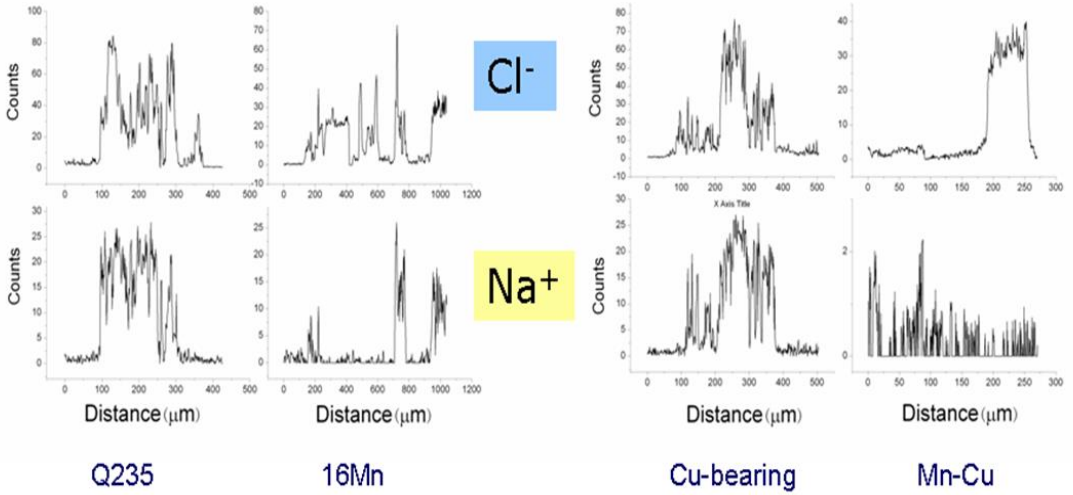

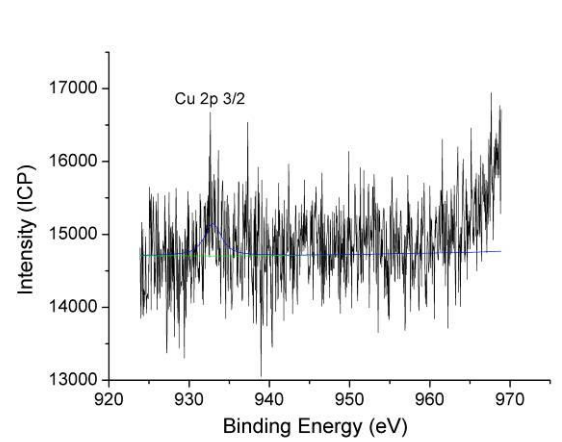

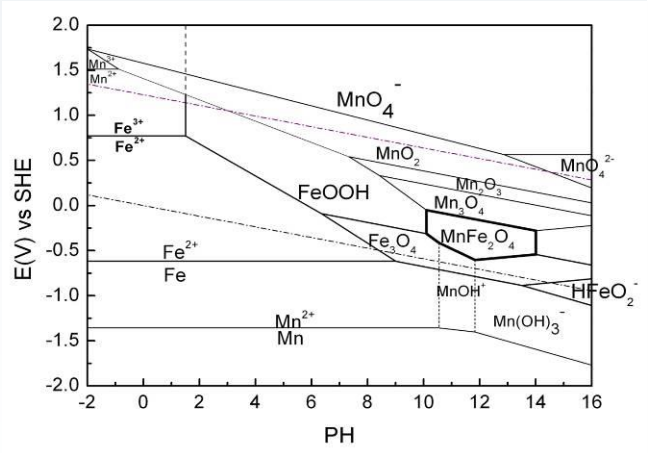

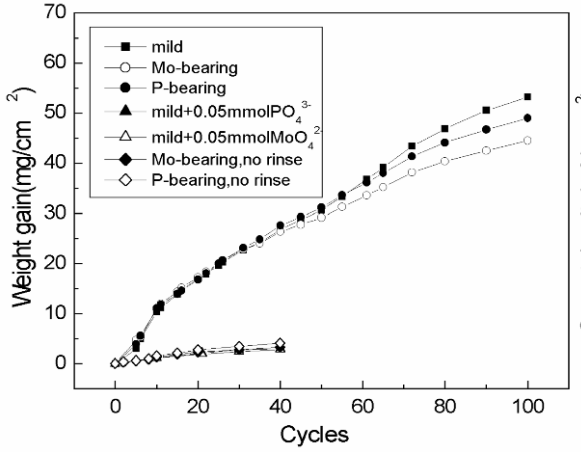

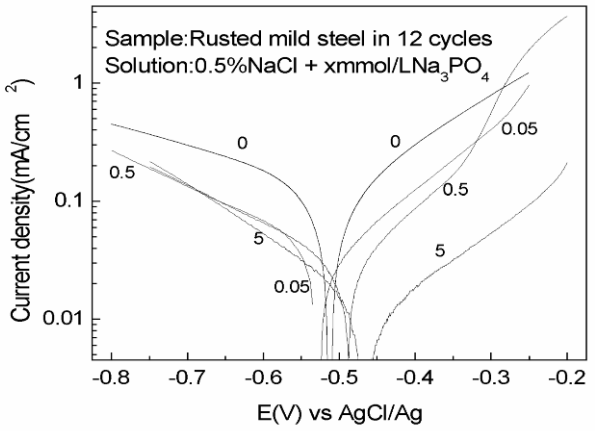

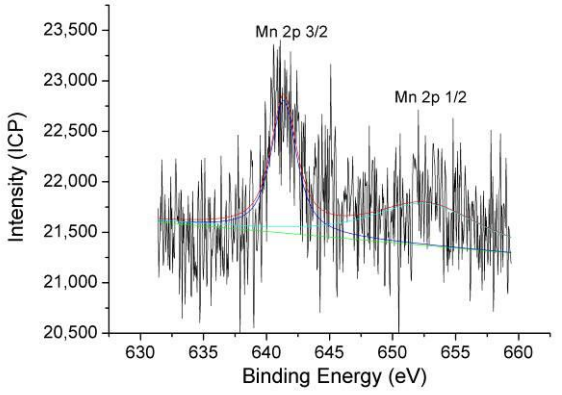

Relationships of rust composition/structure and its properties of weathering

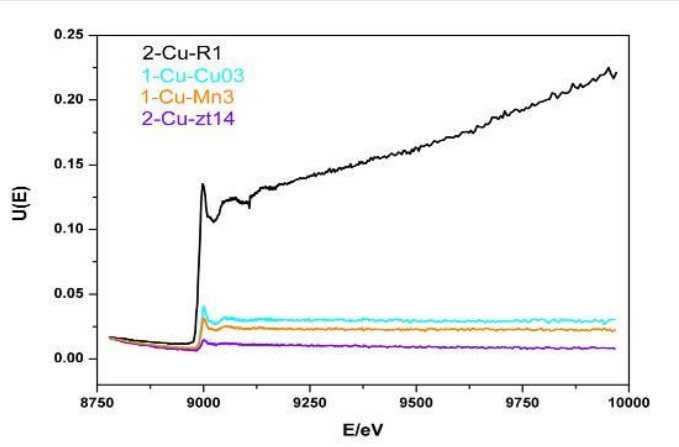

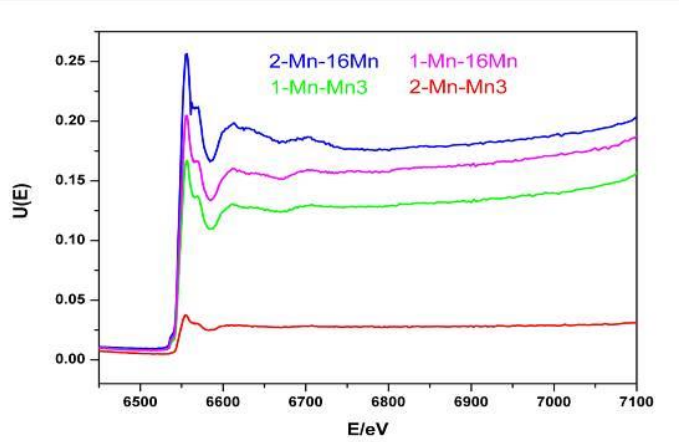

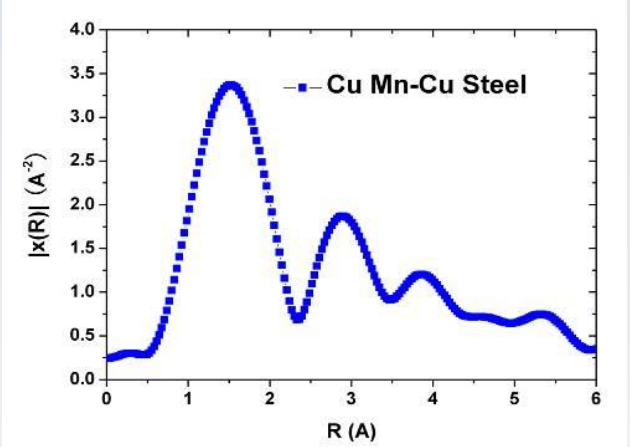

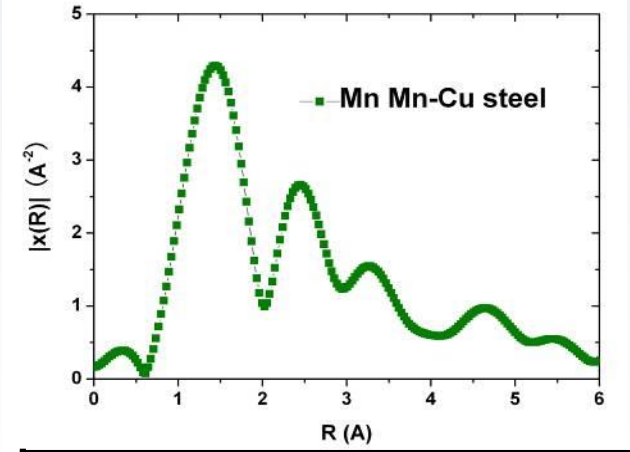

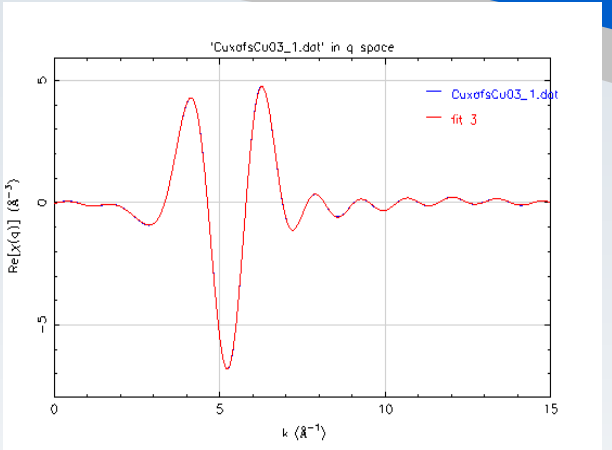

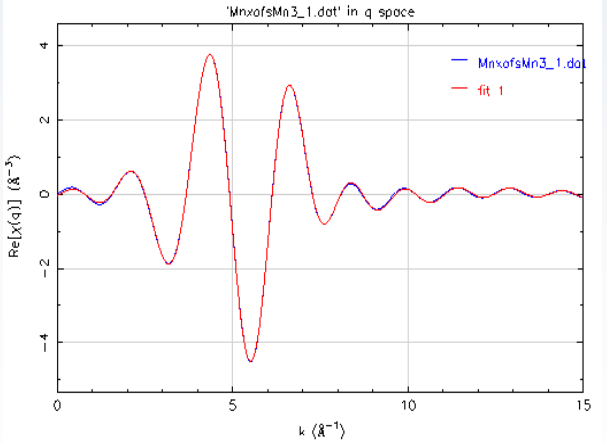

模型：Fe_3O_4

空间群： Fd-3m

	$Cu\text{-}O_x$	$Mn\text{-}O_x$
配位数(x)	4.2	5.8
键长(nm)	0.189	0.189

Atmospheric corrosion evolution

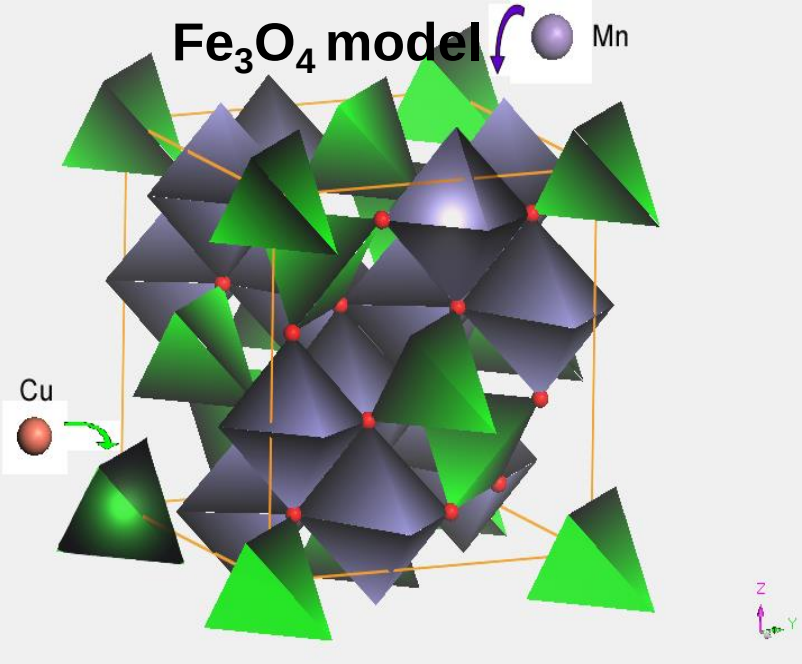

Fe_3O_4: Inverse spinel structure

Unit cell: one tetrahedron and two octahedrons. Three types of Fe atom.

Fe^{3+}: interstitial site in tetrahedron

Fe^{3+}: interstitial site in octahedron

Fe^{2+}: interstitial site in octahedron

- $H_3PO_4 = H_2PO_4^- + H^+$; $pK_1=2.12$
- $H_2PO_4^- = HPO_4^{2-} + H^+$; $pK_2=7.20$
- $HPO_4^{2-} = PO_4^{3-} + H^+$; $pK_3=12.36$

1. PO_4^{3-} and HPO_4^{2-} have strong complex action with H^+, and can lower the dissolution of H^+ to rust layer, leading to the suppressed cathodic process;
2. PO_4^{3-} can form non-soluble phosphate with the dissolved metal ions.

Synergetic principles of Mn and Cu: Cu atom is located in interstitial site in tetrahedron of the crystal of Fe_3O_4, replacing one Fe^{3+}, leading to localized $Cu(I)O_4^{2-}$. The negative charge can be attracted with Mn^{2+} in the rust due to Kulun force, and can repel the penetration of Cl^- in the electrolyte to inner rust layer, leading to the lowered corrosion rate and lower contents of Cl and Na in the rust.

Mechanism of Ni on weathering resistance

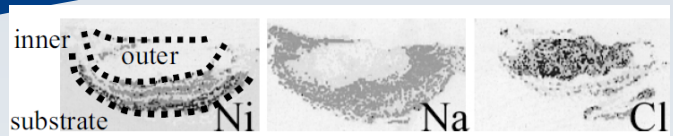

Figure 2 Compositional mapping of the cross-section o the rust in a black (high concentration) - white scale.

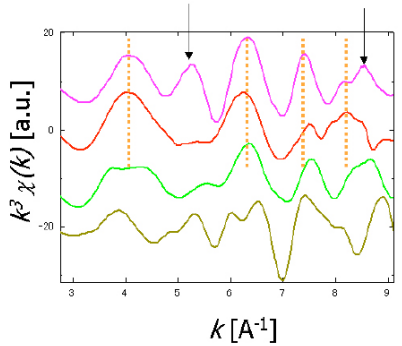

Figure 3 XAFS spectra in the form of $k^3\chi(k)$, where k is the wave number and $\chi(k)$ is the oscillation term: NiC at Ni K-edge (bottom), α-FeOOH at Fe K-edge, the inner layer at Ni K-edge, Fe_3O_4 at Fe K-edge (top) Some of the spectra were shifted along the x-axis fo comparison.

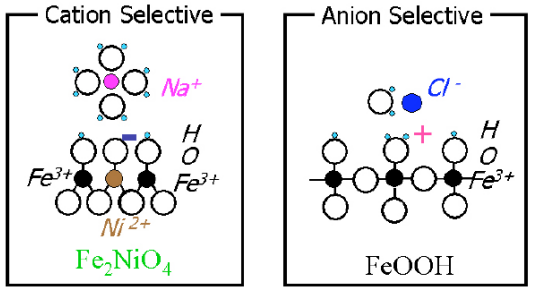

Fig. 4 Schematic diagram of the interface between a rust and a solution on it, when pH of the solution is low.

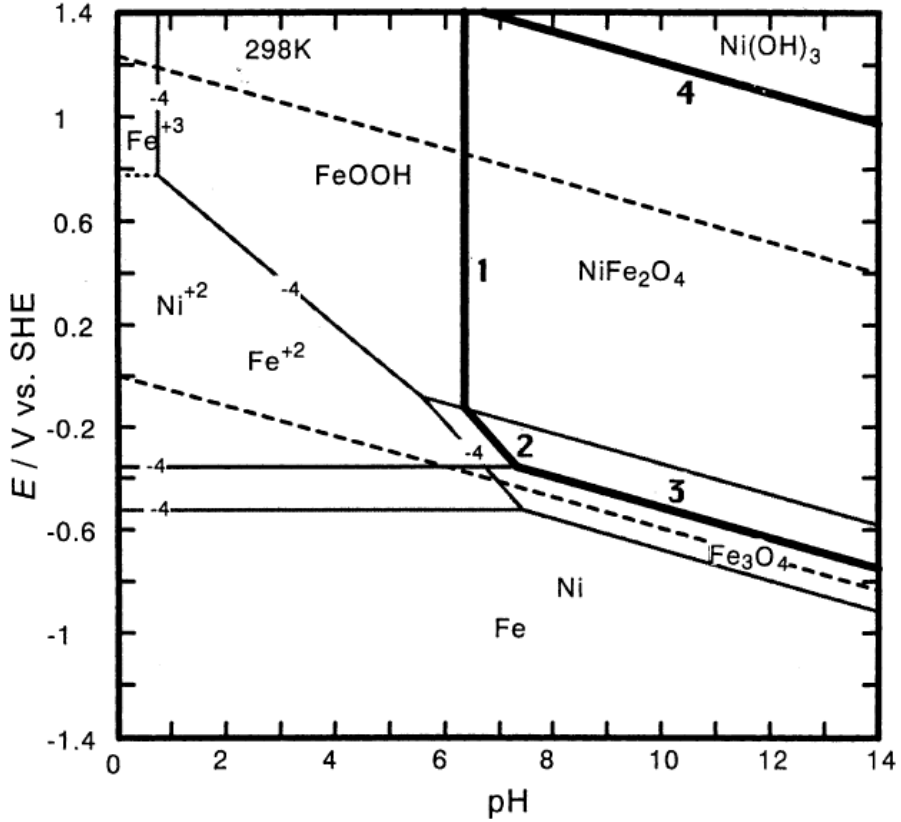

Fig. 1. Potential (E)–pH diagram for Fe–Ni binary system assuming $[Fe^{2+}] = 10^{-4}$ and $[Ni^{2+}] = 10^{-4}$ mol/kg. (1) $H^+ + 1/2\,NiFe_2O_4 = 1/2\,H_2O + 1/2\,Ni^{2+} + FeOOH$, (2) $e + 4H^+ + 3/2\,NiFe_2O_4 = 2H_2O + 3/2\,Ni^{2+} + Fe_3O_4$, (3) $e + H^+ + 3/8\,NiFe_2O_4 = 4/8\,H_2O + 3/8\,Ni + 2/8\,Fe_3O_4$ and (4) $e + H^+ + Ni(OH)_3 + 2FeOOH = 3H_2O + NiFe_2O_4$.

Mechanism of Cr on weathering resistance

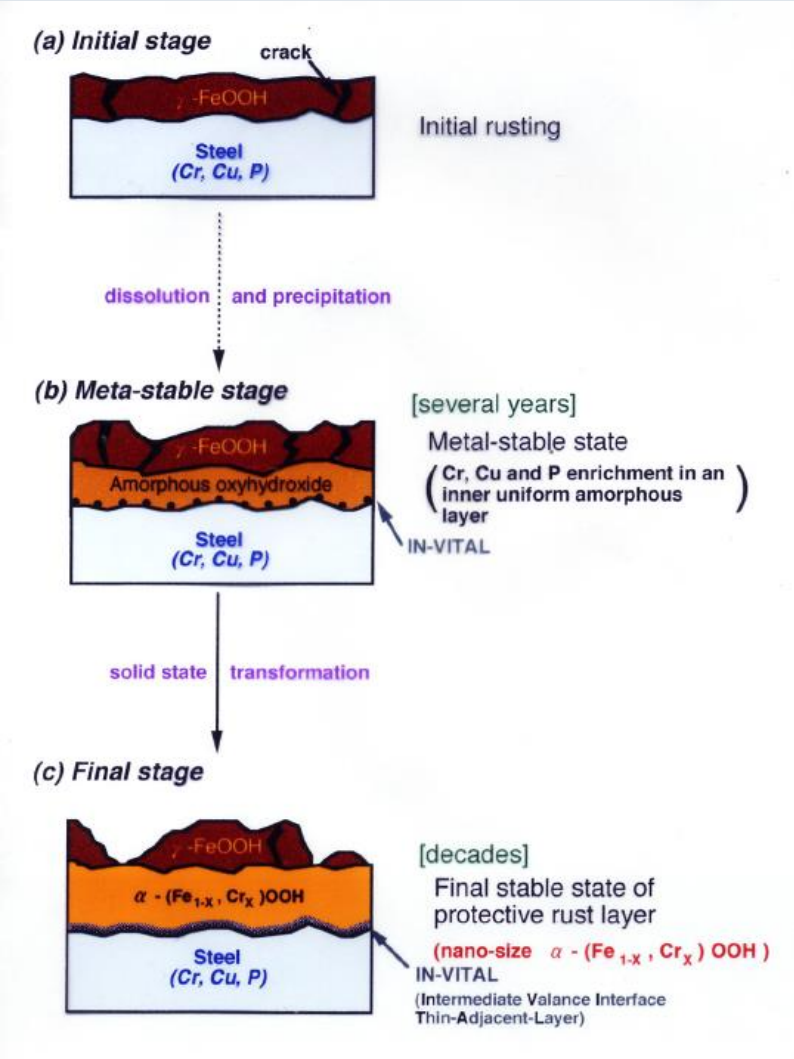

Protective Rust Layer

Dense Aggregation

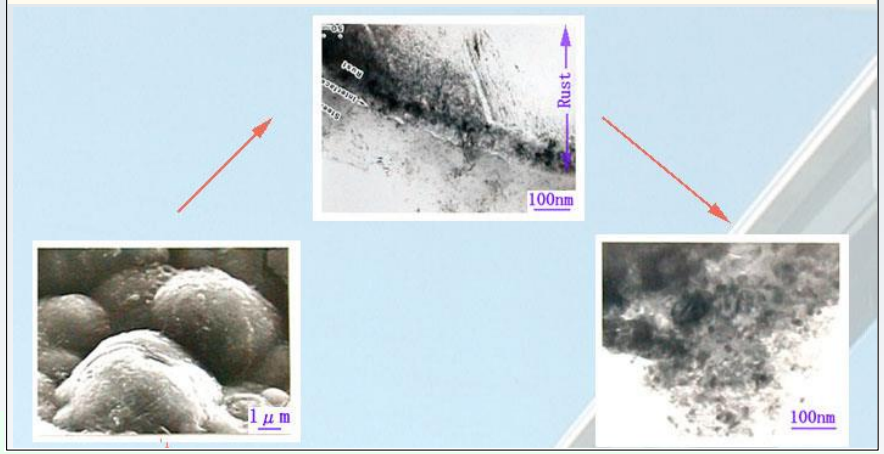

Cation Selectivity

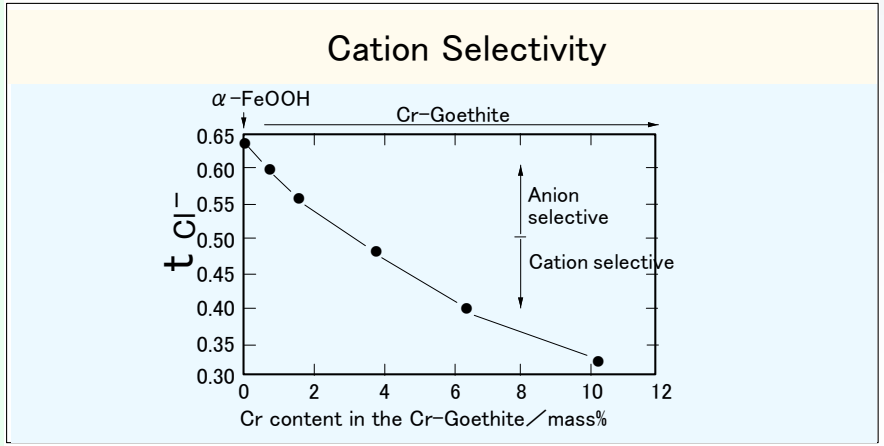

M.Yamashita

Mechanism of Cr on weathering resistance

Radial Structure Function around Cr and Fe

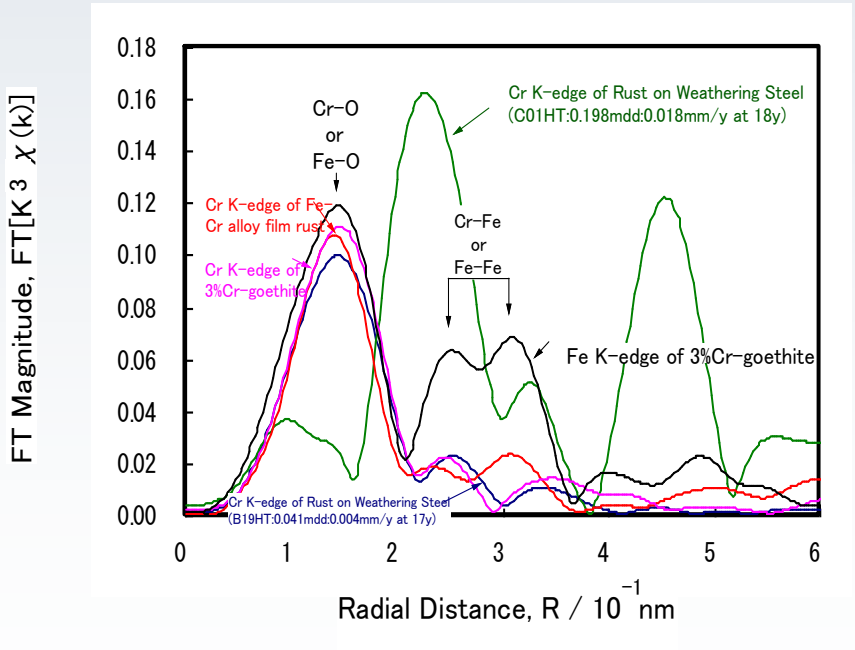

Fig. Fourier transform of the EXAFS spectrum, i.e. radial structure function, of the rust layer of the Fe-5mass%Cr alloy film and the weathering steel rusts at Cr K-edge and those of the artificial 3mass%Cr-goethite powder at Fe and Cr K-edges measured by using PF synchrotron radiation X-rays.

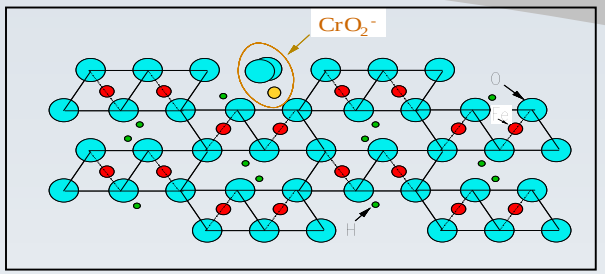

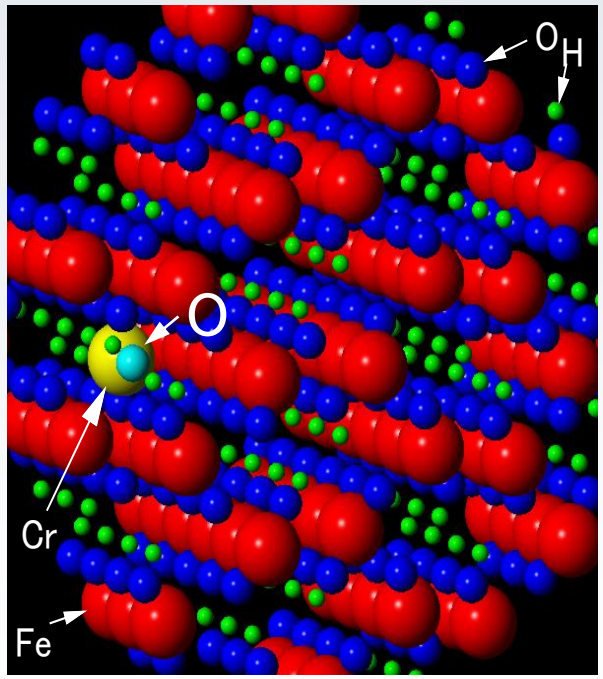

Fig. Schematic of atomic arrangement of Cr-goethite with considering interstitial Cr.

M.Yamashita, H.Konishi, J.Mizuki and H.Uchida(2001)

Models of alloy elements on weathering resistance

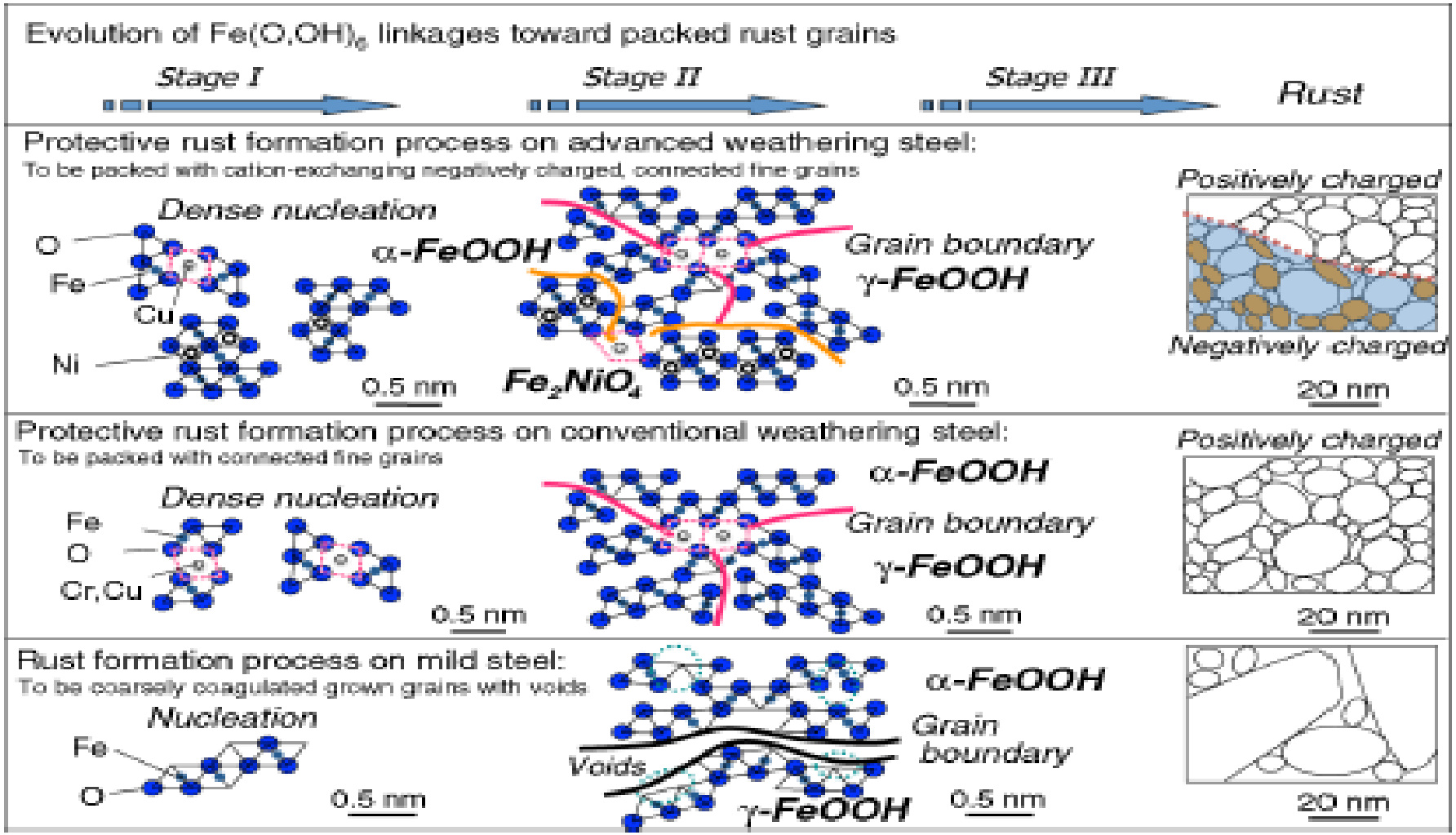

FIGURE 6. *Two dimensionally illustrated models for nanoscale rusting processes on plain carbon, conventional, and advanced weathering steels derived from results and views in terms of various in situ and ex situ advanced analyses.*

www.imr.cas.cn

Weathering steel used for bridge

表 1 美国桥梁用钢标准与钢号概况

AASHTO[3] M270[3 3]	ASTM A709	类似于 ASTM[3 3 3]	屈服强度（最小）/ ksi (MPa)	抗拉强度（最小）/ ksi (MPa)	钢板厚度范围 / mm
36	36	A36	36 (248)	58 (400)	≤101.6
50	50	A572	50 (345)	65 (449)	≤101.6
50W	50W	A588	50 (345)	70 (485)	≤101.6
HPS50W	HPS50W		50 (345)	70 (485)	≤101.6
HPS70W	HPS70W	A852	70 (485)	85 (585)	≤101.6
100	100	A514	100 (690)	110 (760)	≤64
			90 (621)	100 (690)	>64, ≤101.6
100W	100W	A514	100 (690)	110 (760)	≤64
			90 (621)	100 (690)	>64, ≤101.6
HPS100W	HPS100W		100 (690)	110 (760)	≤64

3：AASHTO为美国国家高速公路和运输协会的缩写 ；3 3：除非有其它规定 ，否则强制进行韧性检验 ；3 3 3：在化学成分和抗拉性能方面相类似 ，韧性检验根据补充段落可选择进行。

GB/T4171 -2008	ISO4952 -2006	ISO5952 2005	EN 10025-5 2004	JIS G3114 2004	JIS G3125 2004	ASTM A242M	ASTM A588M	ASTM A606	ASTM A871M		
Q235NH	S235W	HSA235W	S235J0W S235J2W	SMA400AW SMA400BW SMA400CW							
Q295NH											
Q355NH	S355W	HSA355W2	S355J0W S355J2W S355K2W	SMA490AW SMA490BW SMA490CW			GradeK				
Q415NH	S415W										
Q460NH	Q460W			SMA570W SMA570W							
Q500NH											
Q550NH											
Q295GNH										B	09CuPCrNi
Q355GNH	S355WP	HSA355W1	S355J0WP S355J2WP		SPA-H	Type1				A	09CuPCrNi
Q265GNH											
Q310GNH					SPA-C			Type1			

高强度耐候桥梁钢的发展与现代冶炼和轧制技术和装备的发展密切相关。2000年已纳入国标GB/T4172的焊接结构耐候钢包括：Q235NH、Q295NH、Q355NH和Q460NH。1989年武钢研制的NH35q曾试用于京广路运司河桥梁，但未推广使用。

TABLE 1

Example of Stipulated Chemical Compositions (mass%) for Weathering Steel

JIS G 3114 (Conventional Weathering Steel)[A]

Code		C	Si	Mn	P	S	Cu	Ni	Cr	Other	v
SPA-H SPA-C		≤0.12	0.20–0.75	≤0.60	0.070–0.150	≤0.035	0.25–0.55	≤0.65	0.30–1.25	—	
SMA-400 (A/B/C)	W	≤0.18	0.15–0.65	≤1.25	≤0.035	≤0.035	0.30–0.50	0.05–0.30	0.45–0.75	May add Mo, Nb, Ti, V, Zr, etc. Total: ≤0.15	—
	P		≤0.55				0.20–0.35	—	0.30–0.55		
SMA-490 (A/B/C)	W		0.15–0.65	≤1.40			0.30–0.50	0.05–0.30	0.45–0.75		
	P		≤0.55				0.20–0.35	—	0.30–0.55		
SMA-570 (A/B/C)	W		0.15–0.65				0.30–0.50	0.05–0.30	0.45–0.75		
	P		≤0.55				0.20–0.35	—	0.30–0.55		

JIS G 3114 Equivalent[B] (Nickel Added Advanced Weathering Steel[C])

Code	C	Si	Mn	P	S	Cu	Ni	Cr	Other	v
SMA400W MOD V12	≤0.18	≤0.35	≤1.40	≤0.035	≤0.035	0.50–1.00	0.70–1.70	≤0.08	—	≥1.20
SMA490W MOD V12		≤0.55	≤1.60							
SMA570W MOD V12										
SMA400W MOD V15		0.15–0.65	≤1.25			0.30–0.50	2.50–3.50			≥1.50
SMA490W MOD V15			≤1.40							
SMA570W MOD V15										

[A] For conventional weathering steels, such as JIS G3114 SPC and SMA, v values are not specified, but are normally calculated by Equation (2) to be around 1.0.

[B] All material properties of Ni added advanced weathering steels comply with JIS G3114 SMA except chemical composition, so that MOD is added in SMA codes.

[C] As examples for this article, chemical compositions and codes for nickel added advanced weathering steels with v values guaranteed by a maker are selected. More of different stipulations are provided by the other makers.

Weathering steels used for bridges

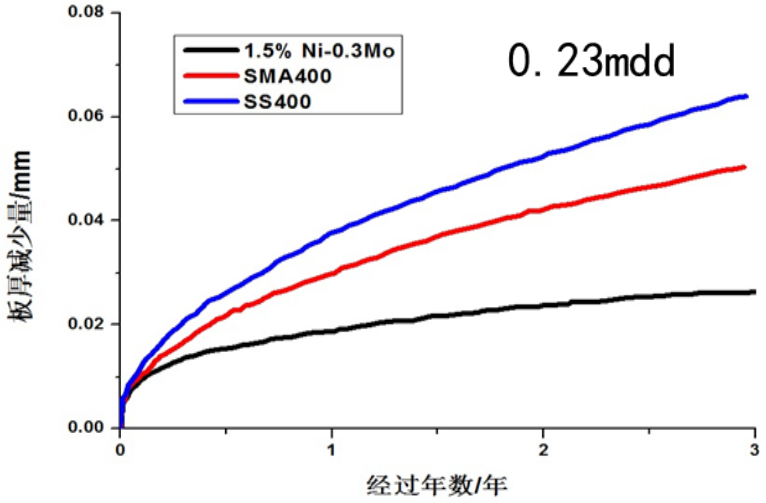

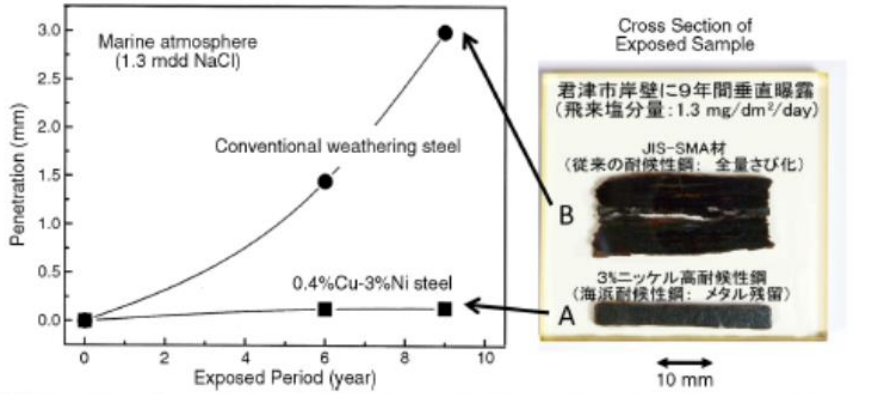

FIGURE 5. *Results of a 9-year exposure test at 10 m away from a wharf in terms of conventional and nickel-added advanced weathering steels. The former was almost rusted out while the latter remained mostly metallic.*

Table 1 Chemical compositions of Ni added weathering steels

Steel	Thick-ness (mm)	Chemical composition (mass%)										Mechanical properties				
		C	Si	Mn	P	S	Cu	Ni	Mo	C_{eq}*1	P_{CM}*2	YS (N/mm²)	TS (N/mm²)	El (%)	$_{v}E_{0}$*3, $_{v}E_{-5}$*4, (J)	$_{v}T_{S}$ (°C)
JFE-ACL400 Type1	12	0.04	0.30	0.57	0.032	0.003	–	1.42	0.30	0.27	0.13	291	460	34	373	−59
JFE-ACL490 Type1	50	0.07	0.32	0.71	0.033	0.002	–	1.45	0.32	0.33	0.16	358	515	38	281	−43
JFE-ACL570 Type1	75	0.07	0.26	0.74	0.029	0.004	–	1.48	0.31	0.32	0.16	532	625	32	270	−50
JFE-ACL400 Type2	50	0.02	0.27	0.32	0.011	0.003	0.37	2.60	–	0.15	0.10	355	460	40	355	−35
JFE-ACL490 Type2	50	0.02	0.29	0.92	0.006	0.005	0.37	2.68	–	0.26	0.14	445	528	39	388	≦−80
JFE-ACL570 Type2	50	0.02	0.34	0.98	0.013	0.002	0.39	2.61	–	0.27	0.14	523	637	32	390	≦−80

*1 C_{eq} = C + Mn/6 + Si/24 + Ni/40 + Cr/5 + Mo/4 + V/14, *2 P_{CM} = C + Si/30 + Mn/20 + Cu/20 + 60/Ni + Cr/20 + Mo/15 + V/10 + 5B,
*3 ACL400 Type1, ACL490 Type1, ACL400 Type2, ACL400 Type2, ACL490 Type2, *4 ACL570 Type1, ACL570 Type2

Weathering steel used for bridge

Corrosion acceleration test of MnCuMo steel in a simulated industrial environment

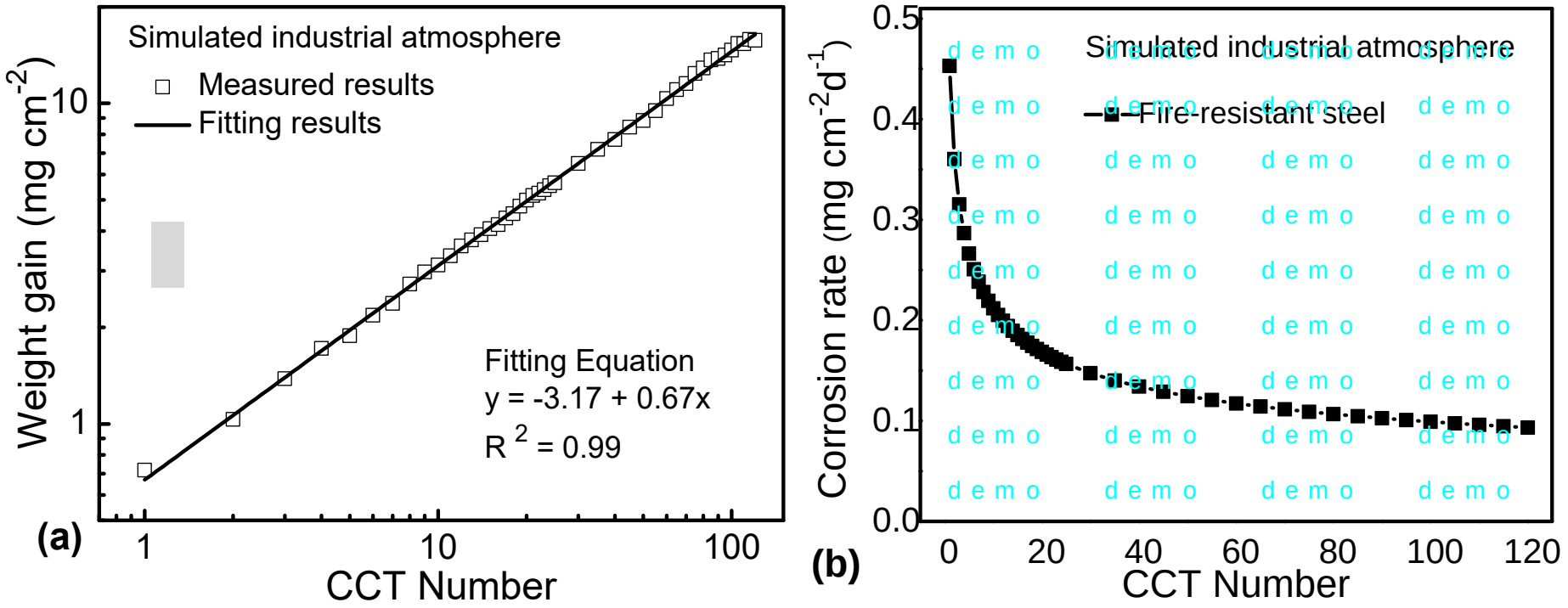

MnCuMo钢在模拟工业大气中的腐蚀动力学：(a) 腐蚀增重曲线，(b) 腐蚀速度曲线

Weathering steel used for bridge

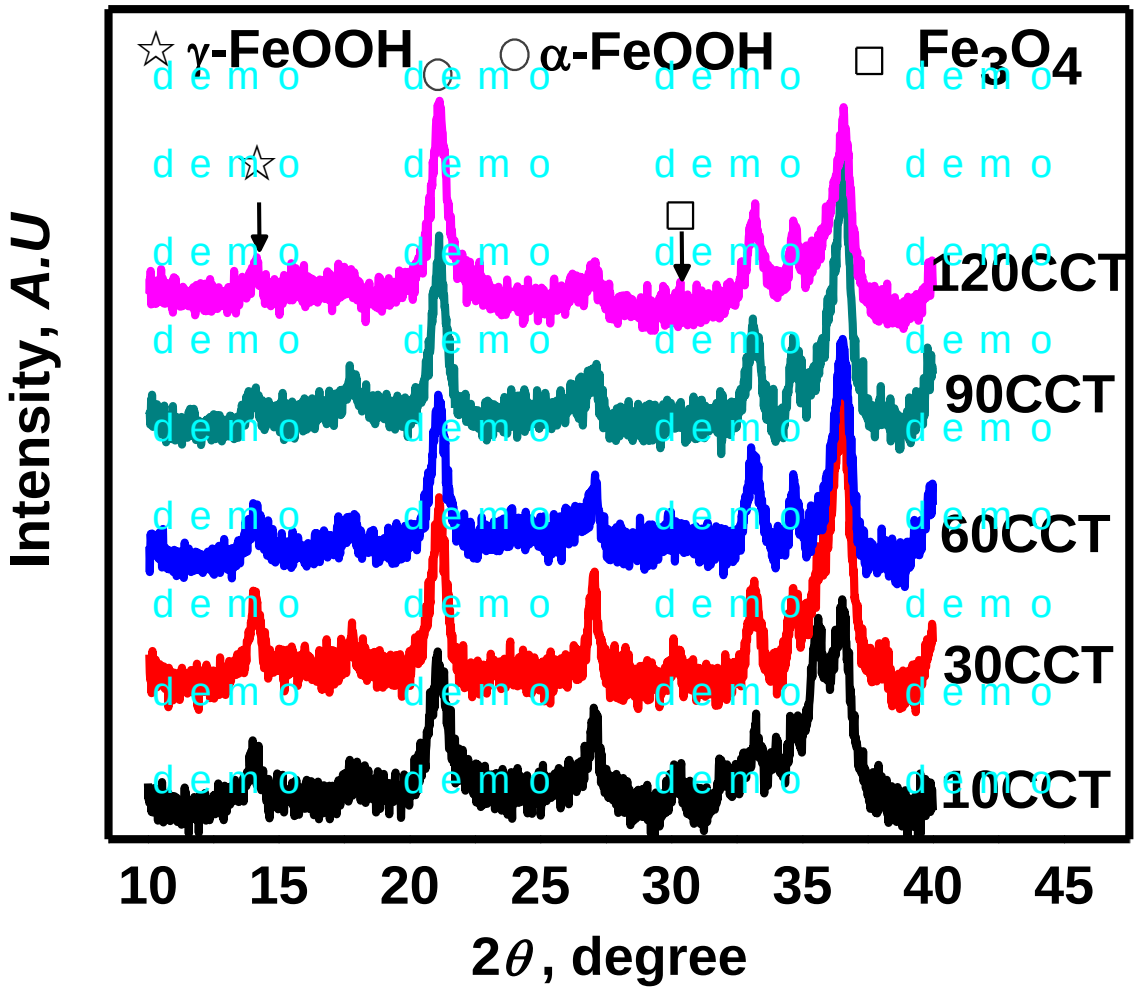

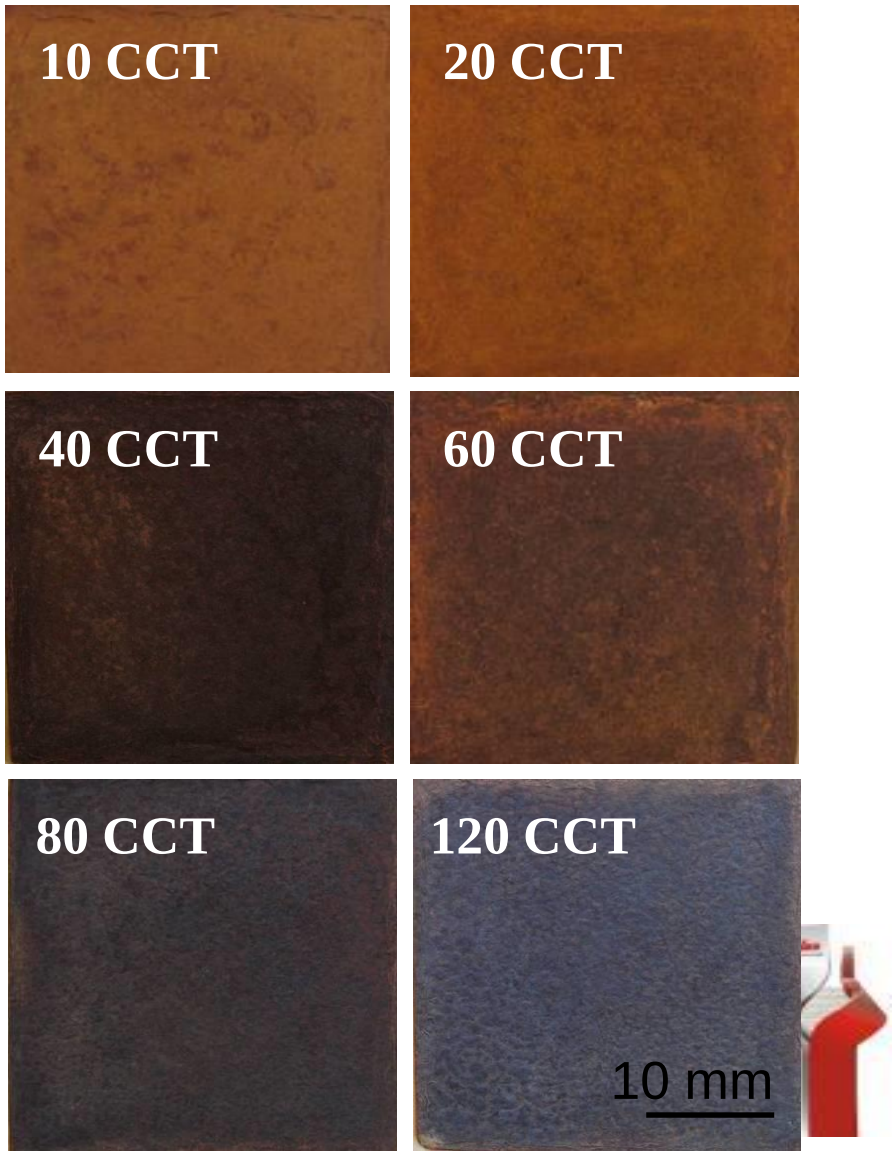

Stabilization methods of the rust layer

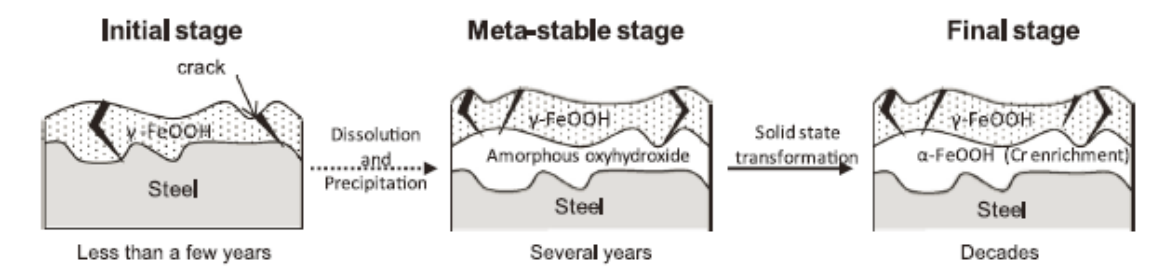

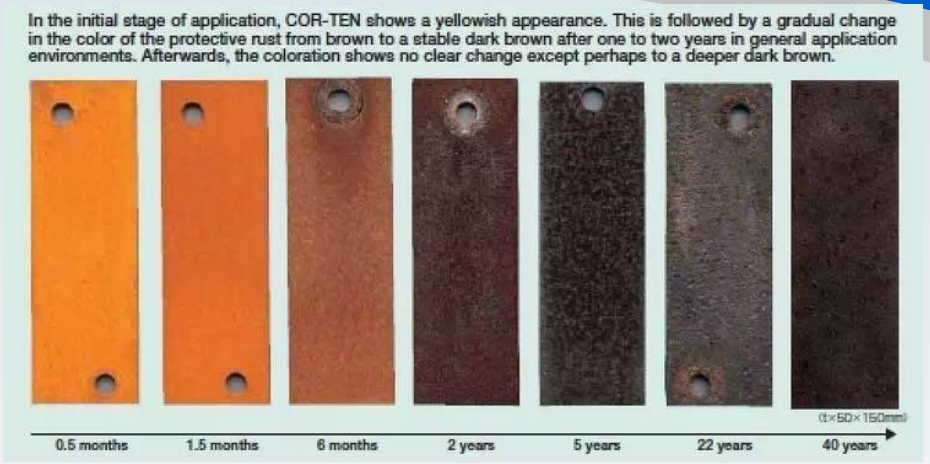

Under natural atmosphere condition, it takes 4~15 years to be stabilized, which caused a bigger thickness loss

- Rust compositions
  - atmosphere
    1. industrial(SO_2)：α-FeOOH、γ-FeOOH
    2. coastal(Cl^-)：β-FeOOH
    3. industrial-coastal (SO_2+ Cl^-)：upon the content of SO_2
  - Alloy elements
    - Cu: Fe_3O_4; Ni: Fe_3O_4;
    - Cr: α- FeOOH; Mn-Cu: Fe_3O_4, γ -FeOOH

- Kind of rust and its effect
  1. Slow corrosion：α-FeOOH, Fe_3O_4
  2. Promote corrosion：γ-FeOOH, β-FeOOH
  3. Protection index (PAI)：α/γ* = (α-FeOOH+Spinel)/(β-FeOOH+γ-FeOOH)

Yamashita, M., Corr. Sci., vol. 36, pp. 283-299, 1994； W. Ke, J.H. Dong, Acta Metal. Sin. 46 (2010) 1365-1378； L. Hao,, J.H. Dong, W. Ke, Corros. Sci. 58 (2012) 175-180.

Stabilization methods of the rust layer

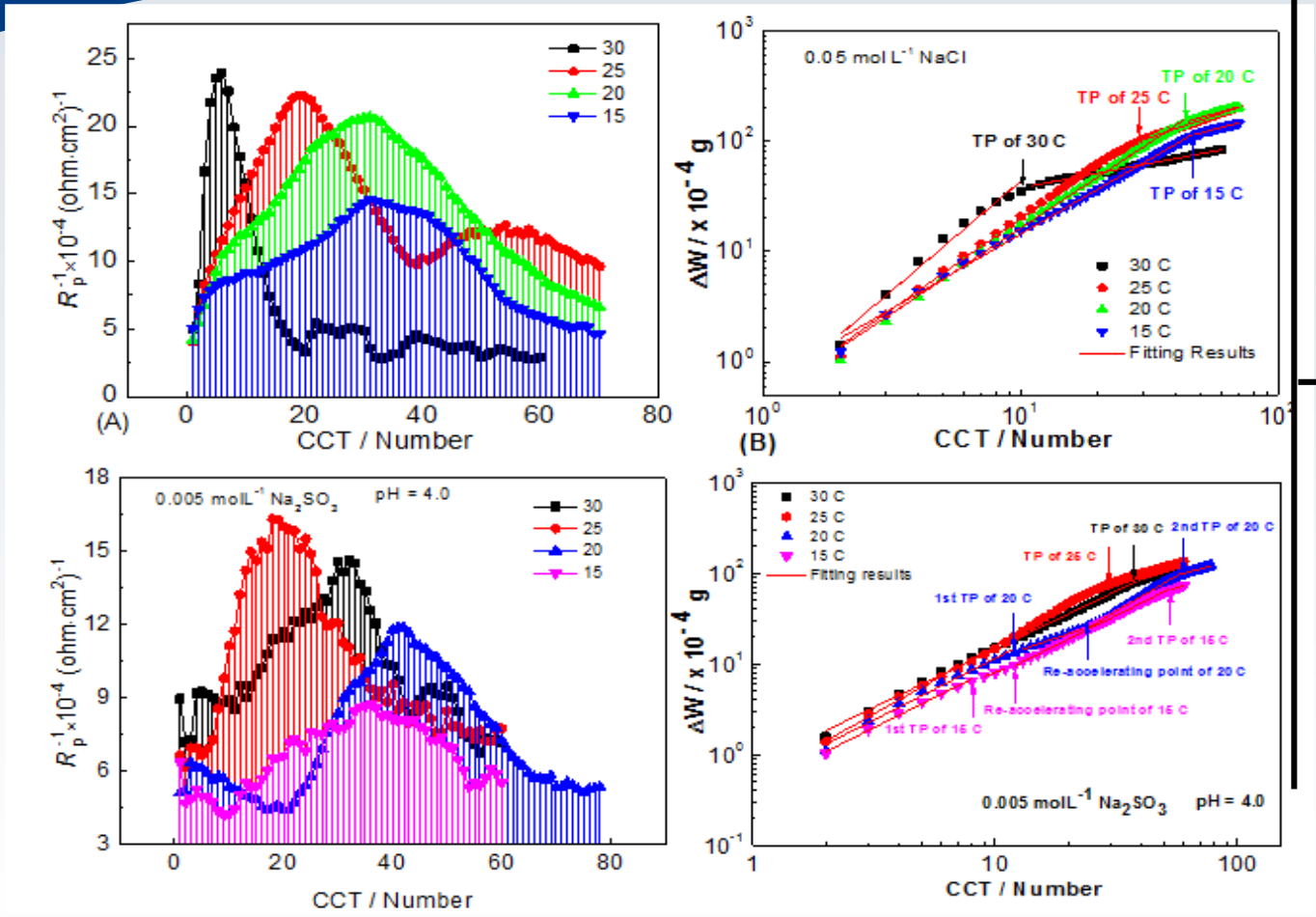

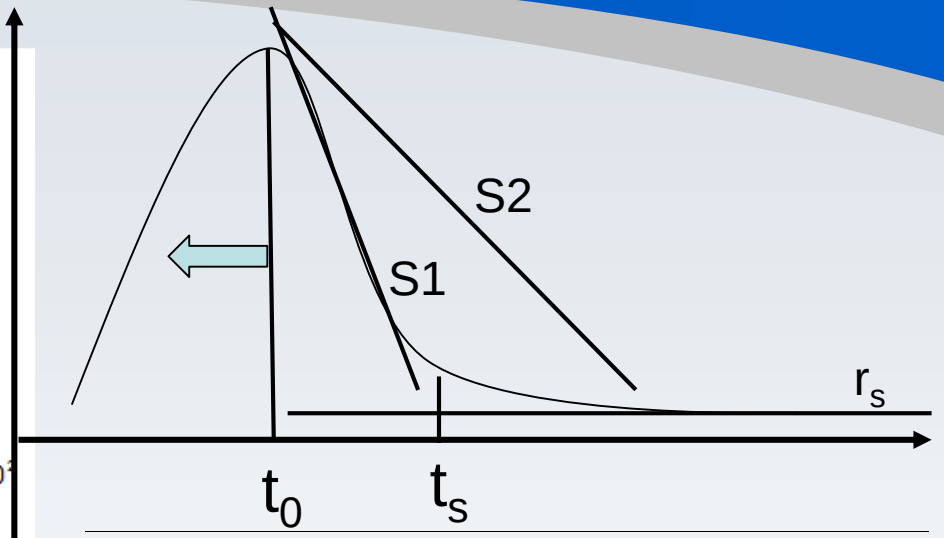

	5d	10d	20d	30d
pH=5				
pH=7				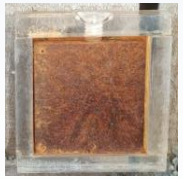
pH=8		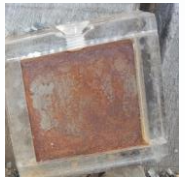		

Stabilization methods of the rust layer

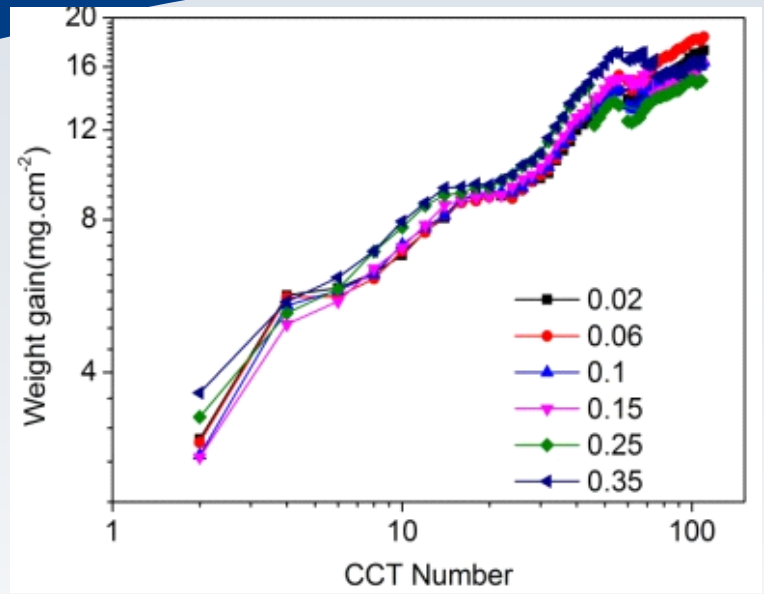

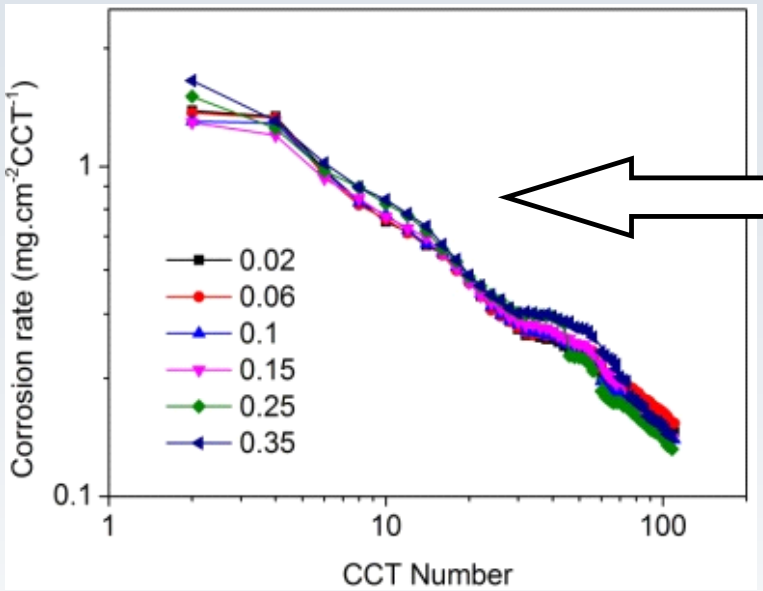

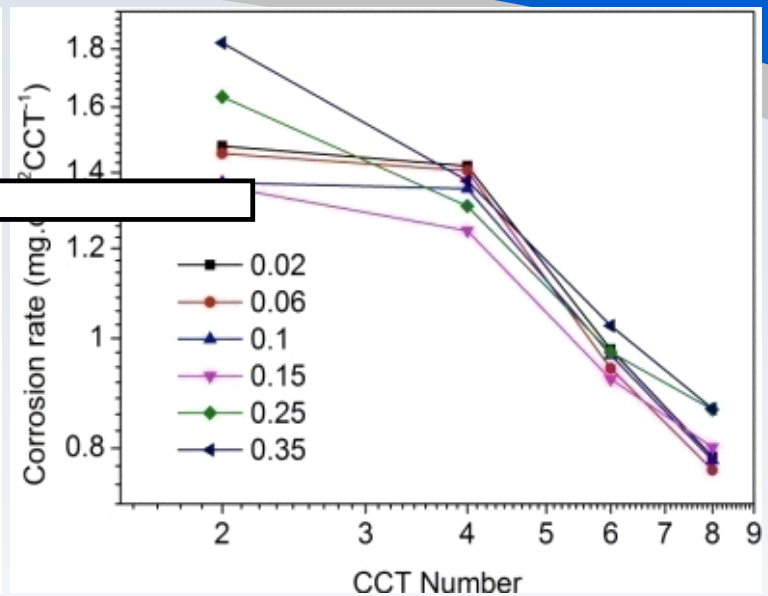

加药结束后的样品　2d　4d　10d　20d　30d　40d

Summary and outlooks

- We introduced the corrosion types of steel rail sections, which are Crevice corrosion, atmospheric corrosion, dissimilar metal contact corrosion
- Studied results for weathering steel applied to bridges are mainly introduced，possibilities of applying to rail manufacture should be existed.
- Steel rail with both wear-resistance and corrosion resistance should be the development focus to prolong the service life of rails.

感谢您的关注！

www.imr.cas.cn

Thank you for your attentions